Transferred Graphene as a Conductive Layer on a Thin Alumina Membrane

Investigating the Feasibility to use Graphene as Conductive Layer in a Timed Photon Counter

Thijs ten Bruggencate

TU Delft

Transferred Graphene as a Conductive Layer on a Thin Alumina Membrane

Investigating the Feasibility to use Graphene as Conductive Layer in a Timed Photon Counter

by

Thijs ten Bruggencate

in partial fulfillment of the requirements for the degree of

Master of Science
in Applied Physics

at Delft University of Technology
to be defended publically on Friday December 6th, 2019 at 3:00 PM

Supervisor:	Prof. dr. ir. Harry van der Graaf	Nikhef, TU Delft
Daily Supervisors:	Dr. Violeta Prodanovic	TU Delft
	M. Sc. Hong Wah Chan	TU Delft
Thesis Committee:	Prof. dr. ir. Harry van der Graaf	Nikhef, TU Delft
	Prof. dr. ir. Pasqualina M. Sarro	TU Delft
	Prof. dr. Peter G. Steeneken	TU Delft
	Dr. Violeta Prodanovic	TU Delft

TU Delft

Summary

For this Master thesis the possibility was explored to use a monolayer of graphene as conductive layer, instead of sputtered titanium nitride (TiN), on 25 nm thick aluminium oxide and magnesium oxide membranes. These membranes will be used in a new and faster variant of a vacuum electron multiplier (e.g. the Photo Multiplier Tube (PMT)). These membranes should act as transmission dynodes, or tynodes, where electrons are multiplied while interacting when they travel through the membrane and leave the membrane on the other side instead of being multiplied by hitting the surface of a dynode, where secondary electrons are released on the same side. These membranes are constructed using insulators and can charge up, as more electrons leave the membrane than enter. To circumvent this issue a conductive layer is applied on these membranes. The advantage to use graphene over TiN as conductive layer would be that the maximum transmission electron yield is higher and occurs at a lower incoming (primary) electron energy due to the reduced total thickness of the membrane. In order to get graphene on the membranes a wet transfer method of graphene was used where a layer of Poly(methyl methacrylate) (PMMA) was applied to support and the graphene sheet and to make it buoyant.

The adhesion of graphene to alumina membranes proved to be very difficult and on many occasions the graphene was washed away during the removal of the polymer by acetone. The few remaining samples that were produced on both alumina and magnesium oxide membranes, where the conductive layer was successfully applied, had a lower transmission electron yield than the samples coated with a sputtered TiN layer. Sputtered TiN was used as conductive material in this project, before graphene was researched for this thesis. The reason for the lower yield is that the adhesion between the conductive graphene and the membranes was not good enough to conduct electrons vertically in the membranes causing them to charge up. One of the reasons for the poor adhesion is that the membranes are wrinkled and curved due to internal stresses that are caused by the production process. The graphene layer cannot follow these curves due to the way it is applied and only makes contact at the tops of the wrinkles. The primary electron energy, where the (lower) maximum yield was observed, was higher than samples with TiN, while the expectation was that graphene as the conductive layer would lower this energy, due to the reduced thickness. These observations lead to the conclusion that graphene is not a viable replacement for TiN as the conductive layer on these membranes.

The use of TiN deposited by Atomic Layer Deposition (ALD) instead of sputtering was also tested. The samples produced with this method conducted electrons well enough to prevent charging effects in the membranes. The added benefit is that the TiN can be deposited with the alumina layer in a single ALD run and that its thickness can be controlled more precisely. The positive results make ALD TiN a viable replacement for sputtered TiN, but more research should be done to find the minimum thickness of this layer where it is still conductive enough to prevent charging of the membranes.

In order to circumvent the abovementioned adhesion issues, a transfer-free method was developed to create graphene-alumina membranes, where the alumina was deposited on the graphene through ALD, instead of transferring graphene on the alumina. Since copper is used as a catalyst to grow the graphene, this put a lot of constraints on suitable wet etching techniques. This resulted in chemical baths where the temperature control was not ideal, which lead to much longer silicon etch times and loss of wafers. Near the end of the process a silicon oxide layer needed to be removed, but this step was most likely not performed correctly, leaving a thin layer of silicon oxide that blocked chemicals

that should remove a deeper layer to release the membranes. Further testing of these samples fell out of the scope of this thesis and could be researched in the future. In conclusion, it is advisable to etch the silicon earlier in the process when the copper has not been deposited yet. In general the flowchart of this process needs a revision.

Table of contents

1. Introduction

Electrostatic photomultiplier tubes (PMT's) were invented in 1937 and are currently still widely used, because of their ability to amplify signals efficiently with low noise and good time resolution. This is realized by the use of dynodes, on which electrons are multiplied in collision with their surface through secondary emission. Each dynode multiplies the incoming electrons with a fixed gain factor. After these collisions the secondary electrons are accelerated towards the next dynode by a potential difference that is applied between the dynodes. In figure 1 a schematic drawing of a PMT is shown.

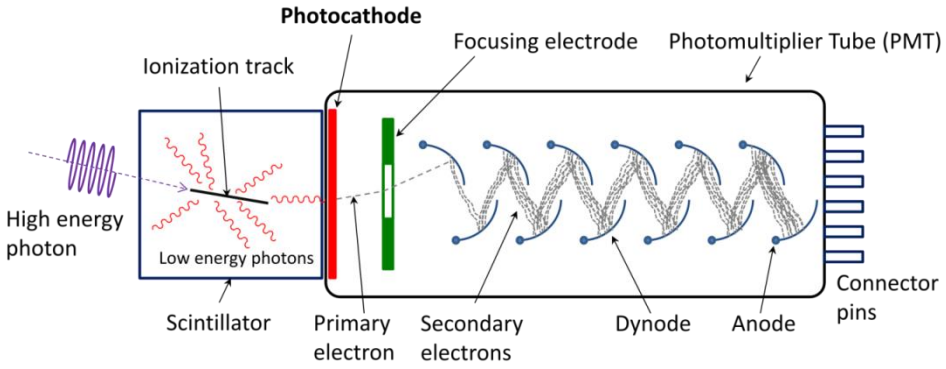

Figure 1. A PMT with a scintillation crystal attached. The dotted lines depict electron paths through the device.

When ionization occurs within the scintillator, low energy photons can be created. When such a low energy photon reaches the photocathode it can be converted in an electron through the photo-electric effect. This electron is focused and accelerated towards the first dynode. The electron collides with the dynode's surface and releases several electrons through secondary emission (Secondary Electron Yield (SEY)). These electrons are accelerated to the next dynode where more electrons are released. This multiplication continues with the same gain factor (the SEY) on every dynode, until the anode is reached where the electrons arrive in large numbers, resulting in an easily measurable signal.

The work conducted in this study is a part of MEMBrane project, which has a goal to develop a new type of photomultiplier, which is called the Timed Photon Counter, TiPC or "Tipsy" for short. Most of the experiments in this thesis are conducted at the Else Kooi Laboratory (EKL) in the Electronic Components, Technology and Materials (ECTM) department and the Micro Electro Mechanical Systems (MEMS) group. Part of the fabrication was also done at Kavli Institute of Nanoscience Delft. In this new photomultiplier curved dynodes are stacked on top of each other in vacuum and the electrons pass through them rather than being multiplied in the regular dynode configuration. This special set of transmission dynodes, or tynodes, is created through MEMS fabrication techniques.

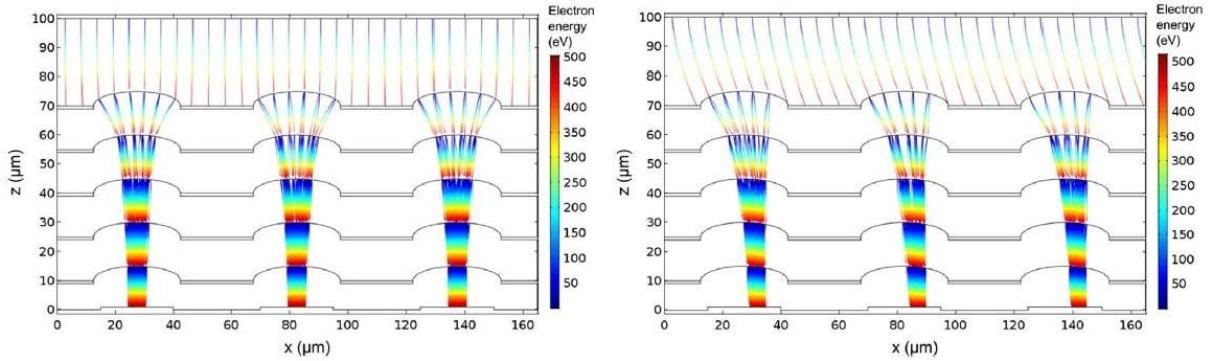

Figure 2. 2D simulated trajectories of electrons through a stack of tynodes. Due to the curvature in the tynodes, the electrons are converging towards the next tynode, making the pathlengths more uniform, relative to convetional PMT's. This has an added advantage that the TiPC also works in a magnetic field as shown in the picture on the right, where the curvature induced by the magnetic field of 1T is countered by the converging effect of the curved tynodes.

These tynodes will be stacked on top of a Complementary Metal Oxide Semiconductor (CMOS) pixel chip and a traditional photocathode will be placed on top. The stack of tynodes will act as an amplifier for an incoming electron in the correct energy range. There are several differences between TiPC and a regular PMT. Firstly, there is a larger potential difference: more than 1 kV compared to 100 V in PMT's (Wikipedia, 2019). Secondly, the distance between the tynodes is much smaller than the distance between dynodes: 300 - 400 µm compared to 5 - 10 mm in regular PMT's (Wikipedia, 2019). Thirdly, the electrons travel in a more uniform, straight path between the tynodes and finally, the curved shape of the tynodes has a focusing effect on the electrons, making it even operational in a magnetic field (figure 2). This means that both the intrinsic gap crossing time and spread in arrival time of the electrons is much smaller than in a regular PMT, giving the TiPC a much better time resolution, possibly as low as 10 ps instead of nanoseconds. This can be very beneficial in for instance medical imaging, like Positron Emission Tomography (PET), where time-of-flight calculations can be performed much more accurately, so that the point-of-annihilation can be determined with greater accuracy. This would enhance the image, while the amount of radiotracers could be decreased.

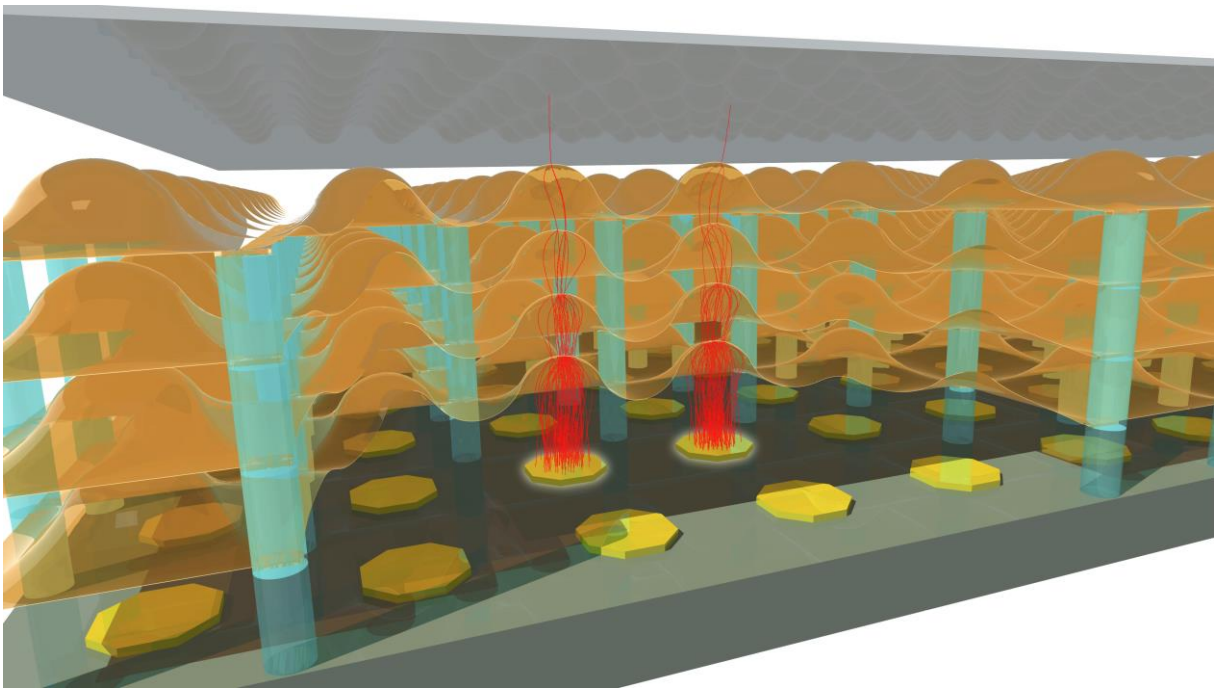

Figure 3. An impression of the final TiPC device with electrons originating from the photocathode on top and multiplying while passing through the several thin membranes or tynodes and finally arriving on the CMOS pixel chip at the bottom.

1.1. Electron Scattering and Secondary Emission

When a (primary) electron enters a material it can interact with the atoms in the material in several different ways. Since an electron is an elementary point particle and the atom mainly consists of empty space, the electron has a high probability to completely miss an atom and fly past it. The electron can pass several atoms without any interaction, but will eventually interact with an atom if the material is thick enough. There are several different interaction possibilities, of which scattering is a large fraction. There are two common ways for an electron to scatter on an atom as is depicted in the figure below.

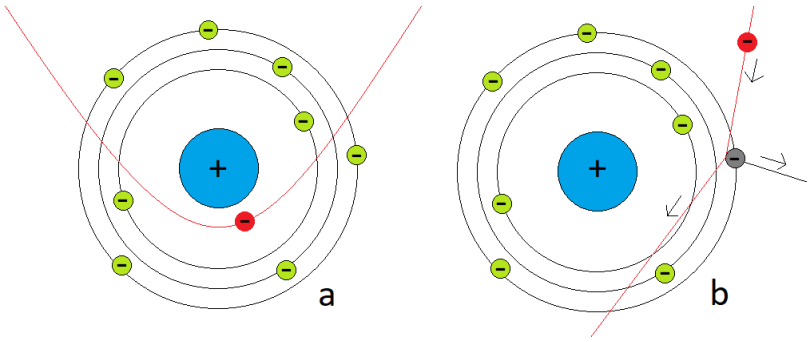

Figure 4. Two different ways an electron can scatter on an atom. a) The primary electron (red) misses the electrons in the electron cloud (green), but comes close to the nucleus (blue) and is scattered back out of the material. The primary electron can also be scattered elastically by the nucleus when it passes slightly further from it, so its path isn't altered so drastically. b) The primary electron collides inelastically with an electron in one of the shells, ejecting it from the atom and thus creating a secondary electron (grey). A high energetic photon can be created when an electron from one of the inner shells is ejected and the vacancy is then filled by an electron on a higher shell.

The primary electron can backscatter when an electron doesn't interact with the electrons surrounding the atom, but comes so close to the nucleus that it is attracted by the electrical field surrounding the nucleus and its path is altered strongly and it can get ejected out of the material on the same side that it entered (figure 4a). It is also possible that the electron scatters elastically on the atom, when it does not get as close to the nucleus and its path is not altered as much as with backscattering. An electron can also collide inelastically with electrons surrounding the atoms, where its path is altered slightly and the electron it collided with is ejected from the atom (figure 3b). There can also be an inelastic scatter process where the electron interacts with an electron on the inner shell of the atom and this electron is ejected. This leaves an empty spot that is filled by an electron from a higher shell under emission of a characteristic photon (gamma). Since the electromagnetic force works over a distance and electrons are point particles, there are no actual collisions, but only close encounters where the electromagnetic force becomes very large and changes the momentum of the particles involved.

When a highly energetic electron enters a material it has a certain chance of scattering in these different ways. Generally speaking an electron has fewer interactions when it has a high energy and seems to have a lot of interaction when it slows down, so it has many interactions at the end of its track through the material. This means that when an electron enters a thin membrane its energy should be high enough such that fewer interactions occur at the top side and it loses its energy before it passes through the material, so that many interactions occur at the bottom side of the membrane. (See figure 5). If the primary electron's energy is too low it will have many interactions at the top of the membrane and few secondary electrons will leave the membrane on the bottom.

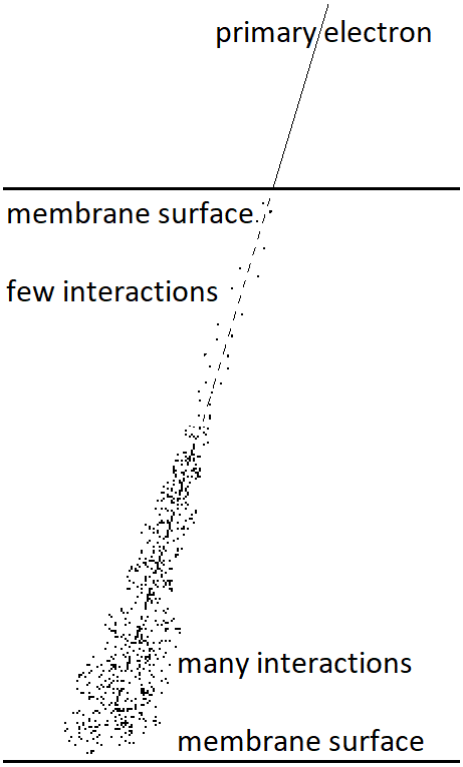

Figure 5. An electron has more interactions at the end of its track, where its energy is low. The secondary electrons released at the end of the track also have low energy, so they will also interact in that region. The interaction pattern in this image would be ideal, because most interactions are in the bottom half of the membrane.

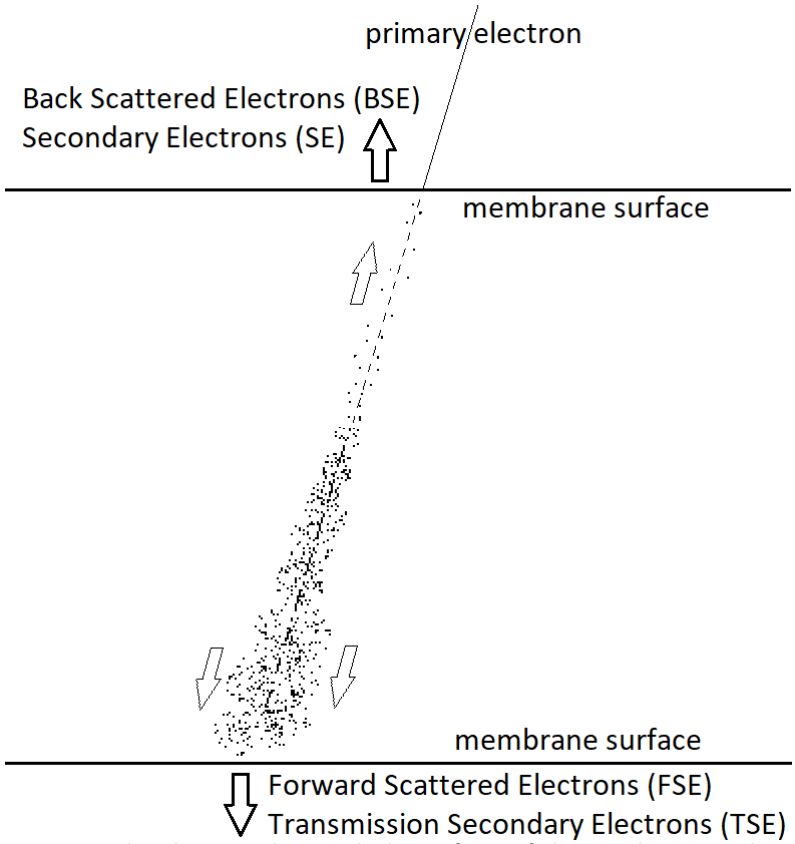

Figure 6. The electrons that reach the surfaces of the membrane can be categorized in four groups: two groups on the side where the primary electron originated and two groups on the other side of the membrane. When an electron has an energy greater than 50 eV it is either a Forward or Back Scattered Electron (FSE or BSE) depending on which side they are released. When an electron has an energy lower than 50 eV, we speak of (Transmission) Secondary Electrons (TSE or SE).

If the energy of the primary electron is too high it will pass the membrane without having many interactions at all and therefore will not create many secondary electrons. This means that there is a certain optimal energy where the most secondary electrons will leave the membrane at the bottom and the electron energy needs to be adjusted to that optimal energy for this device to work well. The exact contribution of the electron groups presented in figure 6 can be found with a special set up inside a scanning electron microscope (SEM) called the Faraday cup. With the SEM the primary electron energy can be precisely adjusted and with sourcemeters the currents, going into and getting out of the sample, can be precisely measured. When this measurement is repeated for multiple electron energy levels a graph can be created and the energy giving the highest transmission secondary electron yield can be determined.

1.2. Tynodes

When a primary electron enters a membrane, it transfers energy to the material electrons and excites them into the conduction band. Since metals have many electrons occupying the conduction band, the energy of the incoming electron is passed on easily to other electrons in the conduction band and the energy is quickly dissipated through thermalization. In insulators, however, the conduction band is not occupied by (many) electrons and the excited electrons are not as likely to scatter by other electrons. The result is that secondary electrons have a (much) longer lifetime in

insulators compared to metals. This also means that the electrons are able to travel larger distances inside the material, increasing their chance to reach the surface and escape from the material.

Due to these described effects, many materials with a high secondary electron yield are insulators. The apparent downside to this is that the emission of secondary electrons leaves vacancies inside the membrane that need to be replenished. As the mobility of electrons and holes is rather low for insulators, the membranes are likely to charge up, because the vacancies cannot be filled fast enough, leaving them unable to emit any extra electrons, due to the change in surface potential. This charging effect is especially critical for membranes, because of their large surface area compared to their low thicknesses, since the distance to an electron reservoir (at the edge of the membrane) is generally quite large. Thereforee we need horizontal conductivity to replenish the electrons that were used in the secondary emission. The solution to this problem was to apply a thin conductive layer on top of the membrane. This will be explained further in the next section and in figure 6.

The chance for an electron to escape the membrane after it reached the surface is mainly determined by the electron affinity of the material and the work function of the surface. When a material has a positive electron affinity, there is a barrier in the energy that the electron can pass when it has enough energy or there is a chance it can tunnel through the barrier. On the other hand a material with a negative electron affinity has no barrier and all electrons can leave the material when they reach the surface. Ideally the membrane would be made from an insulator with a high secondary electron yield and a negative electron affinity.

The preferred material for the membranes was magnesium oxide, MgO, because its secondary electron yield is very high. Also aluminium oxide (alumina, Al_2O_3) was used to create these membranes, because of its high secondary electron yield and because it was a material that could be produced with Atomic Layer Deposition (ALD) in the lab at EKL. MgO could not be deposited in the ALD reactor at EKL. The advantage of ALD is that the thickness of the sample can be controlled very precisely by adjusting the number of cycles in this process, in general 250 cycles were used to create sample with a thickness of 25 nm. Most of the samples in this project were made from alumina and only a few magnesium oxide samples were used, because there was no possibility to create MgO membranes at EKL and they were produced in the United States.

1.3. Conductive Layer

In order to circumvent the charging effects during operation, the application of a thin conductive layer on top of the membranes was proposed (figure 7b). This layer should be applied on the side of the incoming primary electron, so it does not affect the electron affinity and secondary electron yield on the backside of the membrane. Currently the material of choice is Titanium Nitride (TiN), which is

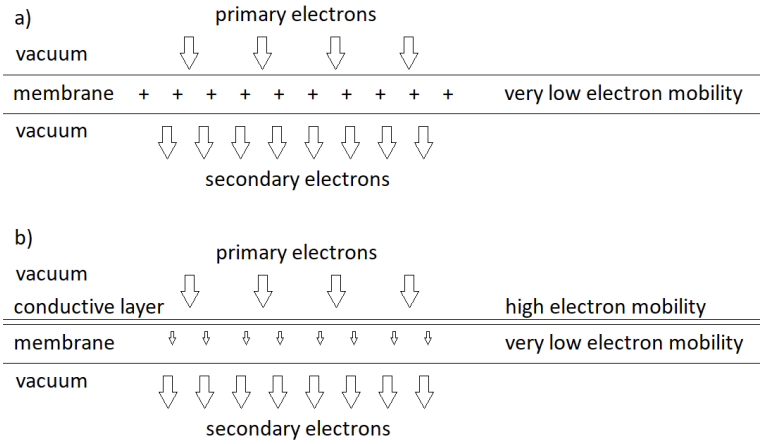

Figure 7. a) When more secondary electrons leave the membrane than primary electrons enter (which is the desired effect), the membrane can charge up, because the electrons in that area are not replenished fast enough to replace the missing electrons. b) The application of a thin conductive layer on top of the membrane can prevent the charging issue, since electrons are easily transported to the area where there is an electron deficit. The electrons can then diffuse or tunnel into the membrane.

conductive at room temperature and can be applied in thin layers by sputtering.

This research focusses on a monolayer of graphene that will be transferred on the membranes as an alternative for the TiN layer. Since a monolayer graphene is only one atom thick (0.345 nm) and TiN needs to be more than 2 nm thick (2.5 nm was generally used) before it conducts enough current for our purposes, graphene is expected to give both a higher yield and also at a lower energy of the primary electron. In the case of graphene, the electron has to travel through only a single layer of atoms and thus has a smaller change to be absorbed in the conductor instead of in the membrane itself. This should result in a higher yield (figure 8). Also, the total thickness of the membrane and the conductive layer is smaller in the case of graphene, 25.3 nm compared to 27.5 nm when using TiN. This means that less material should be passed by the primary electron before it should reach the end of its track (figure 5) and therefore the energy of the primary electron should be lower to find the same optimal TSE yield (figure 8). The applied layer of graphene can also reinforce the membrane making it stronger and less likely to break. This makes graphene an interesting candidate to use as the conductive layer and well worth investigating whether it is a feasible material for this purpose.

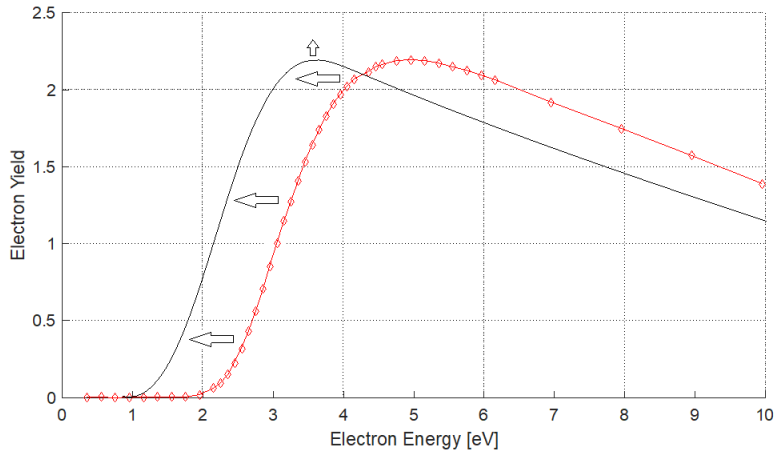

Figure 8. The expected result of using graphene (black line) as the conductive layer on the membranes, compared to 5 nm TiN on 25 nm alumina (previous measurement results, red diamonds). The maximum yield should be reached at a lower energy of the primary electron and the yield should be slightly higher as well since fewer electrons should be absorbed in the conductive layer.

The goal of this research is to find out if graphene works well as a conductive layer on membranes and how it compares with a sputtered TiN layer. The TSE yield and the corresponding optimal primary electron energy (where the TSEY is highest) will be measured in a Scanning Electron Microscope (SEM). These results will be compared with the same measurements conducted on samples with TiN. Also the feasibility of the whole process to create and transfer graphene on the membrane will be evaluated. The production and transfer of graphene is a delicate process that can easily fail, so it was important to find the best order of steps and use the correct chemicals.
In a later stage of the research some experiments were conducted to deposit alumina with ALD on top of graphene, in order to circumvent the transfer process and create membranes that have a stronger bond between the graphene and alumina than the Van Der Waals bond of the transferred samples. Finally some tests were done to deposit TiN through an ALD process instead of sputtering it on the membranes. This would mean that the thickness could be controlled better and had the added benefit that the alumina membranes and the conductive TiN layer could be deposited in a single run in the ALD reactor.

2. Graphene

In this chapter the feasibility to replace TiN by graphene as the conductive layer on the tynodes will be discussed. Graphene is the new 'wonder material' of this century and to fully understand some of its unique properties, some background information will be given first. Then the graphene production method and the quality check that were used will be discussed. After that the transfer method will be described and finally measurements of the resulting tynodes will be presented and discussed.

2.1. Theory - What is Graphene?

Carbon is one of the most important elements found in nature, since it is the backbone of all DNA-based lifeforms. It can be found all around us in wood, steel, plastics and is thereforee omnipresent in our modern society. Pure carbon is found in three distinct generally occurring forms (figure 9). Firstly it can be found as graphite, a black solid that is still used today in a pencil to draw art on paper. In this form the carbon atoms are structured in a hexagonal shape in flat parallel sheets that are stacked on top of each other. The bonds that connect these sheets together are relatively weak compared to the bonds of the carbon atoms inside the sheets. For this reason it is used in a pencil, because these layers can separate due to the force of the graphite that is pressed on the paper. The second form that carbon can take in nature is that of diamond, a transparent solid. This is one of the hardest naturally occurring materials and is used a lot in jewellery because of its refractive properties. The carbon atoms in its crystalline structure are all positioned the same distance apart from each other with four atoms equally distributed around them in a tetrahedron, forming a face centred cubic lattice structure. Thirdly carbon can be found as amorphous carbon, here the atoms are not grouped in a crystalline structure, at least not over large distances, but are connected in a more random way. Amorphous carbon is basically all of the (almost) pure carbon in nature that is not graphite or diamond, like coal, but also left over carbon from incomplete combustion, like soot.

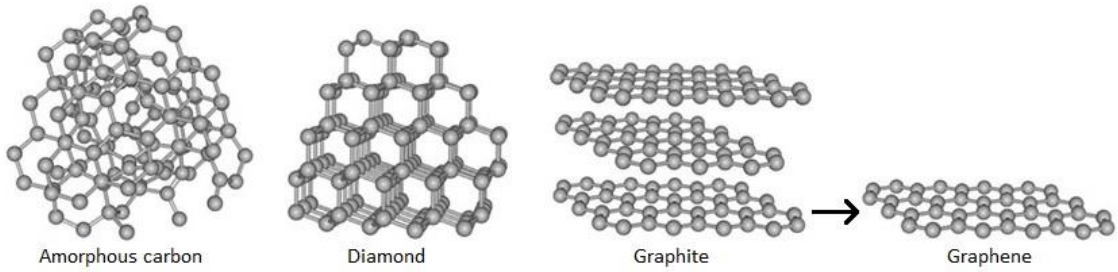

Figure 9. The most occurring allotropes of carbon. Amorphous carbon on the left does not have a structure that repeats over large distances, diamond has a tetrahedral structure that makes it one of the hardest materials. Graphite is made up of sheets graphene that are connected to one another through Van der Waals forces and can be sheered of relatively easily. Graphene, a single sheet of graphite, has a 2-dimensional hexagonal structure, making it a true 2D crystal. (Ehrenfreund & Foing, 2010)

Graphene is a fourth form of carbon that is actually a single layer of graphite with the thickness of one atom, where the carbon atoms form a hexagonal structure in a plane. Graphene can be easily created by using a pencil on paper, where due to the friction with paper, the layers of graphite separate and stay behind. It was first studied in 1962 with electron microscopes where the graphene was supported by metal. It wasn't until 2004 that graphene was extensively studied and isolated, with the scotch tape method, by Andre Geim and Konstantin Novoselov (Novoselov et al., 2004), for

which they received the Noble Price in Physics in 2010. Their work started a new interest in the material and the number of papers regarding graphene rose exponentially from 2004.

Graphene has some interesting physical properties: it is a 2D crystal, something that was believed to be impossible, and it is strictly speaking a semiconductor, however with a band gap of 0 eV (figure 10). Among many other things, this means that it can conduct electricity at room temperature, since thermal excitation of electrons is enough to place electrons in the conduction band. This unique property, that a sheet of material that is one atom thick can transport electrons, makes graphene extremely suitable to replace the conductive layer on top of the membranes in this project.

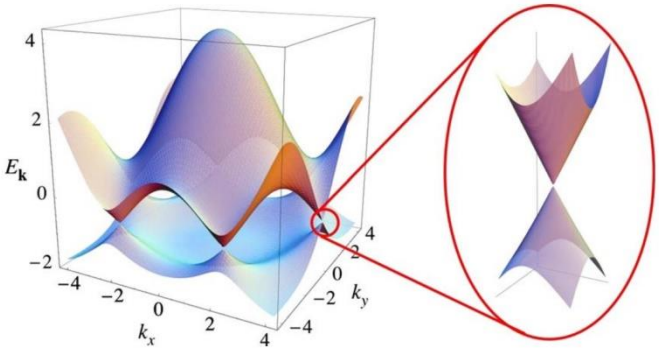

Figure 10. The band structure of graphene in a single unit cell. The energy bands meet in six so called Dirac points in a hexagonal configuration. The Fermi level at T = 0 K can be found where the two bands meet. Since the conduction band is empty and the valence band is completely filled, graphene is a semiconductor with a band gap of 0 eV. (Castro Neto, Guinea, Peres, Novoselov, & Geim, 2009)

To find out why graphene is conductive and diamond is not, even though they consist of the same kind of atoms, we need to investigate how the atoms bond with one another in these materials. Carbon is the sixth element in the periodic table, meaning it has 6 protons and 99% of its isotopes have 6 neutrons as well in its core. In the ground state the electron configuration is $1s^2 2s^2 2p^2$. The electrons in the 2s orbital are located close to the nucleus and do not take part in chemical reactions. The four electrons in the outer shell, occupying the 2s and 2p orbitals are available for reactions. The 2s orbital is approximately 4 eV lower than the 2p ($2p_x$, $2p_y$ and $2p_z$) orbitals, making it energetically favourable for two electrons to occupy the 2s orbital while the other two occupy any of the 2p orbitals. In the presence of other atoms however, it is energetically favourable for one of the 2s electrons to be exited into the 2p orbital in order to form covalent bonds. The energetic gain from such a bond is indeed larger than the 4 eV gap between the 2s and 2p orbitals. See figure 11.

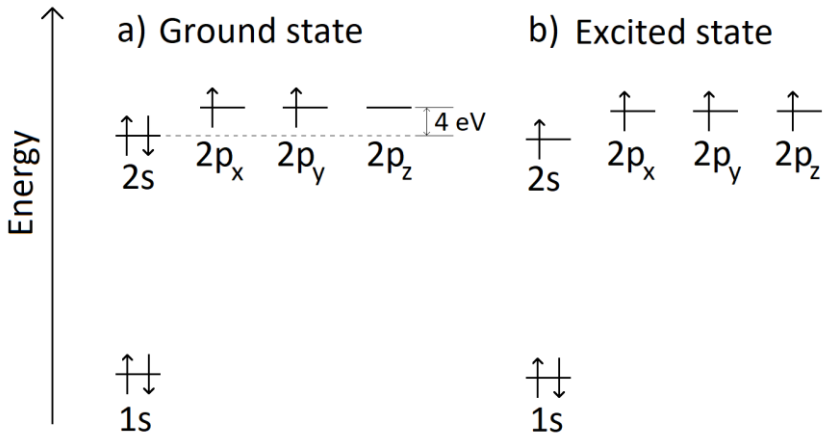

Figure 11. The electron configuration of carbon in the ground state (left) and the excited state (right), where one electron is excited from the 2s to a 2p orbital. This excited state is actually energetically favourite in the presence of other atoms like carbon, hydrogen or oxygen, because the possibility to form covalent σ bonds. (Fuchs & Goerbig)

The unique crystalline structure from the different carbon allotropes arise from sp-hybridisation, a superposition of the quantum states 2s, $2p_x$, $2p_y$ and $2p_z$. In sp1 hybridisation there is a superposition between the 2s state and one of the 2p states. This helps form a strong covalent σ bond between two carbon atoms. The two remaining 2p orbitals are free to form other weaker π bonds. In sp2 hybridisation a superposition between the 2s and two 2p states is formed, resulting in three covalent σ bonds that lie in a plane with 120^o angles between them (figure 12a), resulting in the characteristic honeycomb structure of graphene. Each carbon atom has one electron remaining to form other bonds. This remaining electron is also available to conduct electricity along the surface of graphene. Finally in sp3 hybridisation a superposition between the 2s and all three 2p orbitals is formed resulting in four covalent σ bonds that form a tetrahedron shape, resulting in the crystalline structure of diamond. Because all the electrons of the outer shell are strongly bound in covalent bonds diamond is not an electrical conductor under normal conditions, but is in fact a semiconductor with a band gap of 5,47 eV. (Fuchs & Goerbig)

A material with the same hexagonal structure as graphene is benzene, but it has only a single ring of carbon atoms, and both are examples of sp2 hybridisation. In the case of benzene three covalent σ bonds are formed, two with the neighbouring carbon atoms and the third with the hydrogen atom sticking out of the hexagon. The remaining electron forms a weaker π bond with a neighbouring carbon atom. When the distances between the carbon atoms were first measured, it was expected that the hexagonal structure would not be perfect, because the distance between the atoms in a C=C bond is smaller (0,135nm) than a C-C bond (0,147 nm). However the results yielded that the distance between the carbon atoms in benzene were all the same distance 0,142 nm. Later this was explained by the fact that this average distance was the result of a superposition between the two possible configurations of bonds in benzene. The result of this is that the six weakly bonded π electrons are delocalized around the benzene ring (figure 12c).

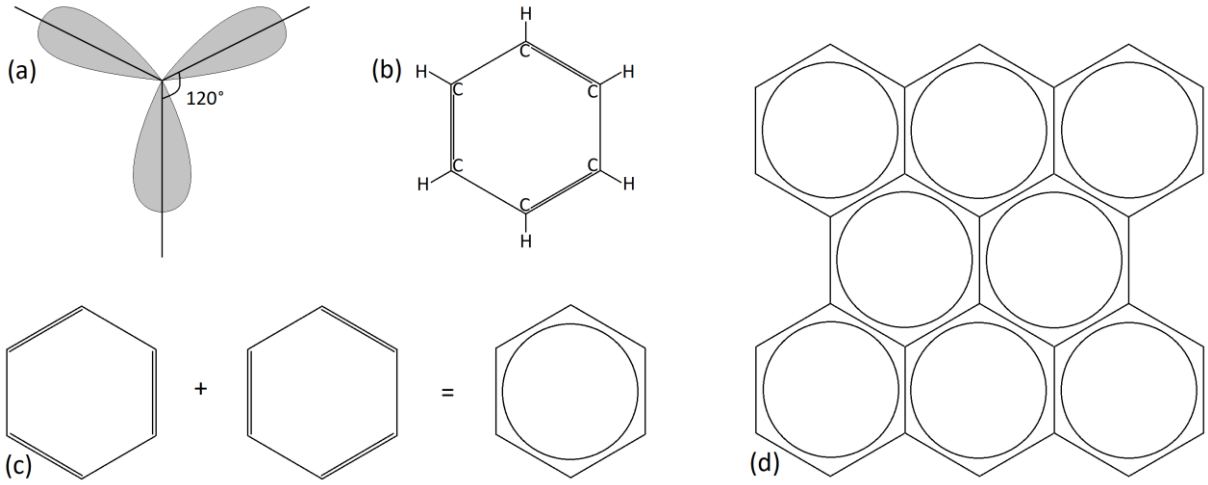

Figure 12. The general shape of the superposition of the 2s and two 2p orbitals (a) that lead to covalent σ bonds where the bubble overlaps with its neighbour. The benzene molecule as it was expected to be formed (b), however it proved to be a superposition of both configurations at the same time (c), where the π electrons are delocalized around the ring. Graphene (d) can be seen as many benzene rings connected to one another without the hydrogen molecules. In this case the π electrons are delocalized over the entire crystal. (Fuchs & Goerbig)

The hexagonal structure of graphene can be seen as an infinite collection of benzene rings, where the hydrogen atoms are replaced with neighbouring carbon rings. The distance between the carbon atoms in graphene is also uniform and 0,142nm. This means that the π electrons are delocalized over the whole sheet of graphene, resulting in the fact that it can conduct electricity.

2.2. Method - Graphene Deposition

The graphene was produced inside a dedicated plasma-enhanced chemical vapour deposition (PECVD) machine, called the Aixtron Black Magic, which was specifically used to grow either graphene or carbon nanotubes with different recipes. The graphene was grown on silicon wafers coated with 500 nm of copper on top of a 200 nm silicon oxide layer, which prevents absorption of the copper into the silicon. The copper acts as a catalyst for methane to break down in hydrogen and carbon, the latter is deposited on the copper.

$$CH_4(g) \xrightarrow{copper} C(s) + 2H_2(g)$$

For this reaction to occur, a high temperature (>700 °C) is required. The resulting hydrogen gas is removed with the carrier gas, Argon. The temperature inside the reactor was varied from 775 °C to 950 °C in order to find the optimum in graphene quality. The goal was to create a monolayer of polycrystalline graphene, with a small amount of defects as this is important for the transfer process. Since mainly the electrical conductivity of graphene was important for its use on the membranes, there is no need to create perfect graphene, some defects are acceptable in its chrystalline structure.

2.3. Results - Testing Graphene Characteristics

The quality of graphene was checked with Raman spectroscopy. With this technique one looks for specific peaks in scattered light from a monochromatic red laser (633 nm). These peaks show up at material specific shifts in wavelength of the scattered light. These shifts in wavelength originate from phonons or lattice vibrations in the material. A phonon can originate from the site where an electron is excited by a photon and part of the energy is transferred. One or several phonons can also come together with an excited electron, giving it more energy before falling back to its ground state. When this behaviour is observed simultaneously in a bulk material and the shift in wavelength is scanned, one can observe peaks in intensity. These shifts in wavelength are coverted in wavenumber (cm^{-1}) to make the results independent of the wavelength of the laser that is being used. The place and relative height and area of these peaks is a good indication for the quality of the material. In the case of graphene these peaks should show up around 1350 cm^{-1} (D), 1580 cm^{-1} (G) and 2700 cm^{-1} (2D). (Childres, Jauregui, Park, & Chen, 2013) The D-peak represents the amount of disorder or defects in the crystalline structure of the graphene, the G-peak arises from C-C bonds which are characteristic of sp2 hybridisation of carbon structures. These structures also show a strong response at the 2D-peak, due to a two-phonon process. For the graphene to be of good quality, the D- peak should be very low or preferably non-existent and the 2D peak should be significantly higher than the G-peak.

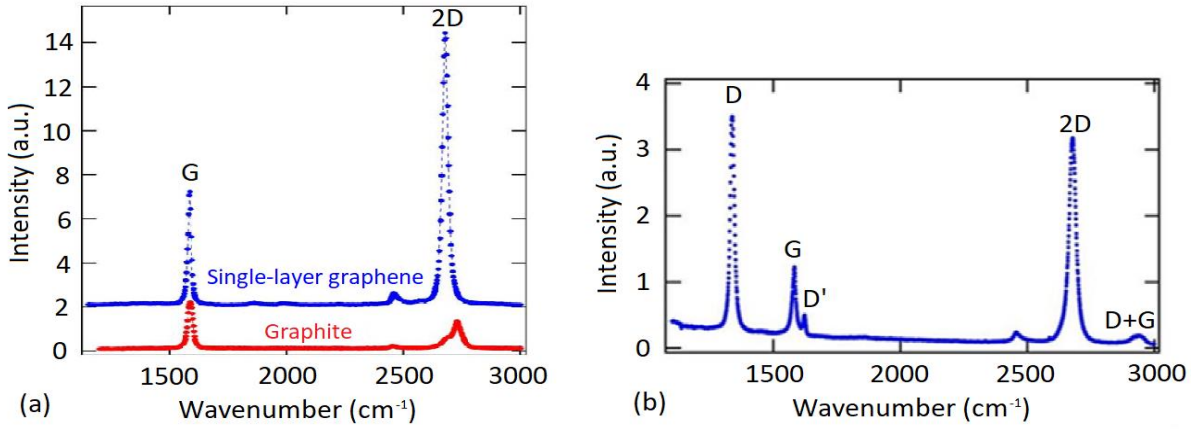

Figure 13. Examples from literature of Raman spectroscopy results of (a) pristine graphene and graphite and (b) results of graphene with a large number of defects in its crystalline structure, where the different peaks associated with defects are visible. (Childres et al., 2013)

In order to evaluate the Raman data, a linear baseline was subtracted and three Gaussians, located at the D-, G- and 2D-peaks, were fitted over the data. This gave information about the relative height and sharpness of the peaks in the form of the full width at half maximum (FWHM). The lower the FWHM of the 2D-peak, the better quality the graphene had. Ideally this number would be lower than 30 cm^{-1}. In figure 14 an example of good quality graphene can be observed. The relative intensity of the G- and 2D-peaks was respectively 1,02 and 6,97. The FWHM of the 2D-peak was 23.0 cm^{-1}, which is excellent.

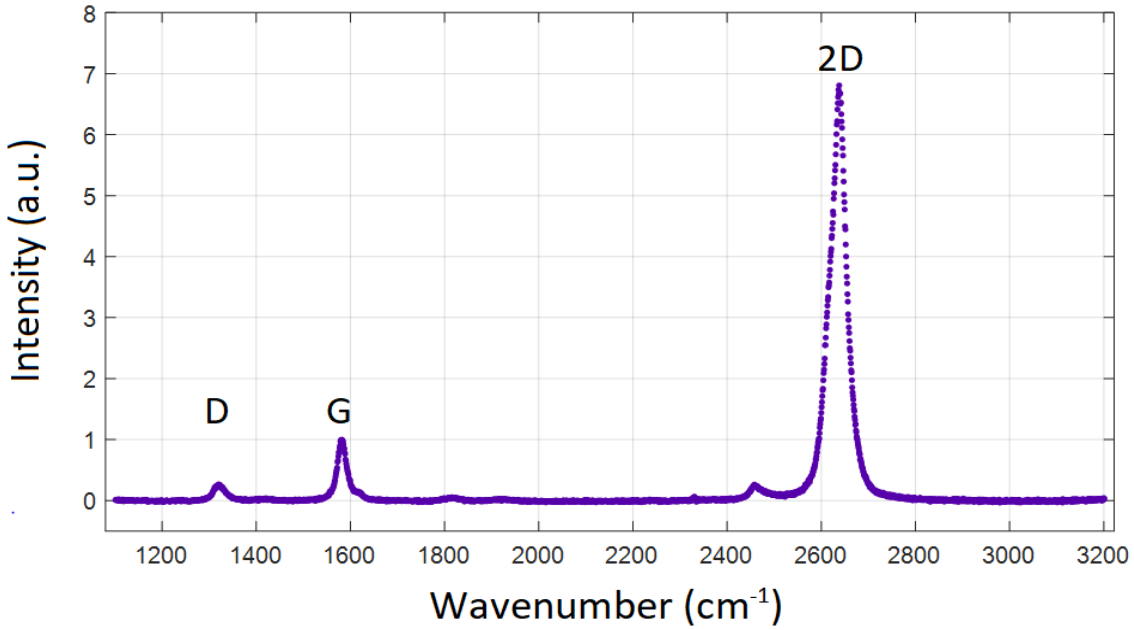

Figure 14. Graphene that is created for this project that is of good quality. The 2D-peak is narrow and much bigger than the G-peak. The D-peak is present but very small, indicating that there are only a few defects in the graphene layer.

Graphene production issues, that will be addressed in the discussion, resulted in a lot of Raman data that showed the graphene quality was not good. In figure 15 an example of such measurement can be seen. Three peaks can still be distinguished, but they are not clearly defined and have the same relative intensity. The FWHM of the 2D-peak also was much wider than desired: 36.7 cm^{-1}. This all indicated that the graphene was of very bad quality or that it was even amorphous carbon.

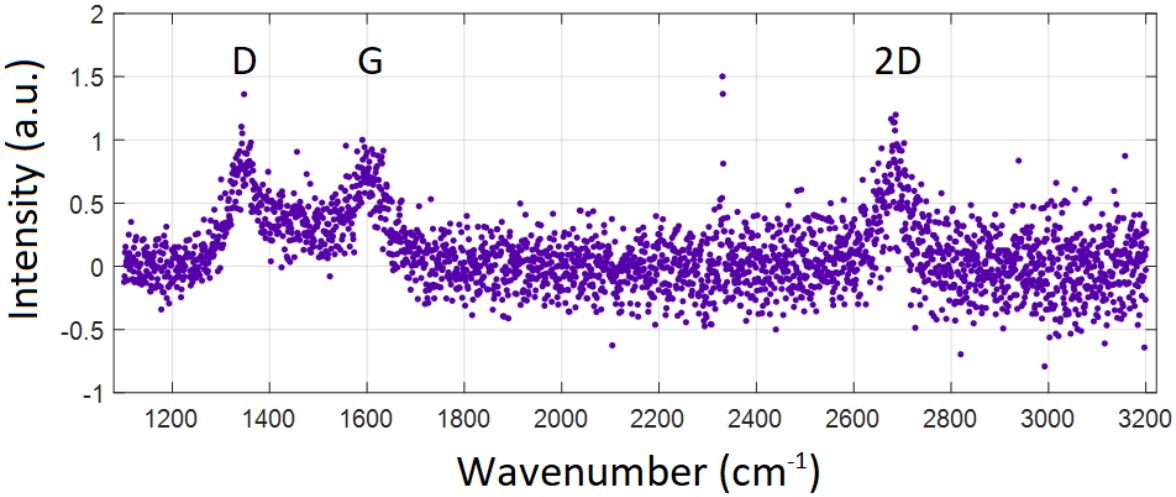

Figure 15. Results from Raman spectroscopy on a sample that has many layers of imperfect graphene or it might even be amorphous carbon. All three peaks are of the same height and smeared out over a large area. This is one example of the bad samples produced due to the defective mass flow controller in the Aixtron Black Magic.

2.4. Method - Transferring Graphene

The graphene was transferred onto the membranes with a wet transfer process. In this process the graphene was supported with a polymer layer, poly methyl methacrylate (PMMA), which prevents the graphene from folding and provides buoyancy so the graphene floats on the surface after it is released from the substrate. The graphene is released by etching away the copper from underneath the graphene using an iron(III) chloride solution. The resulting PMMA-graphene layer floats on the surface of the etchant and could then be scooped, rinsed and finally transferred onto a target substrate, in this case alumina membranes. In figure 16 the production and transfer process is schematically drawn to give an indication of the steps involved. The precise transfer method can be found in Appendix A.

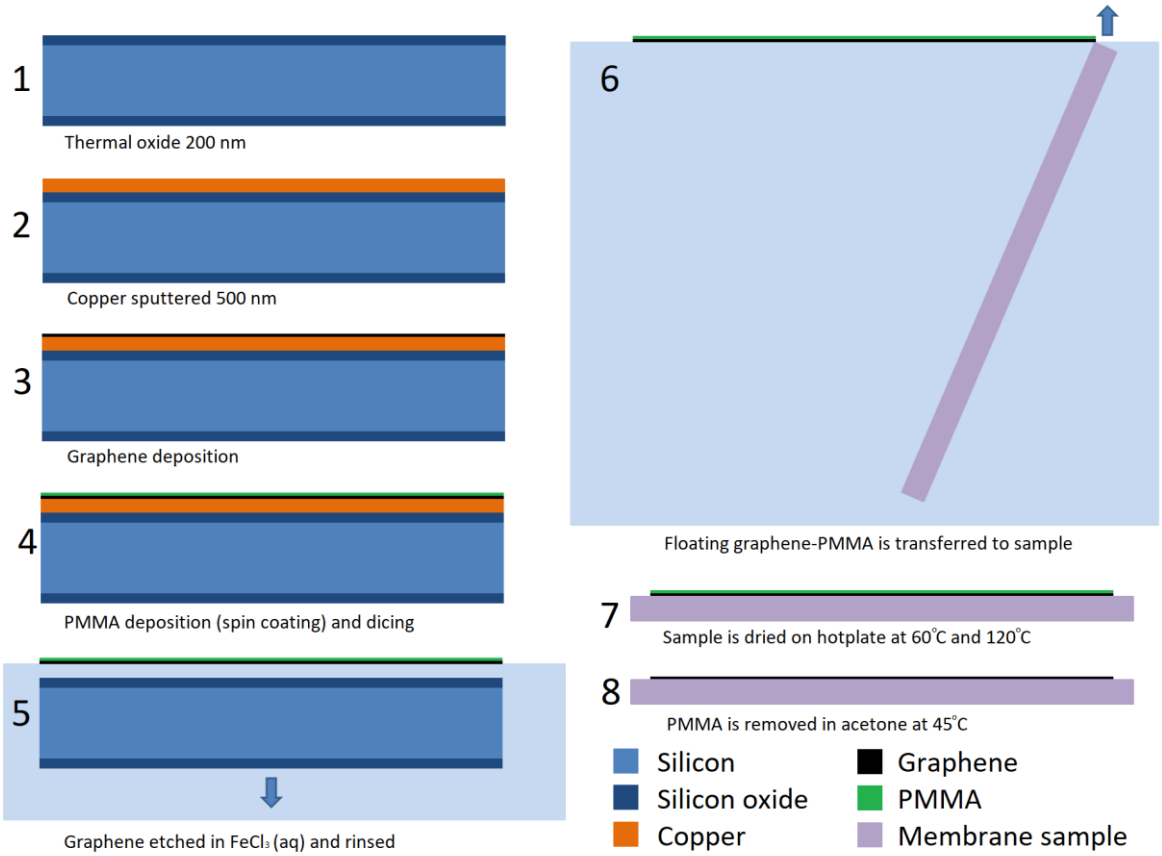

Figure 16. An overview of the graphene production and transfer process. 1) apply silicon oxide, 2) sputter copper, 3) graphene growth, 4) apply PMMA coating, 5) copper etching with Iron(III) Chloride, PMMA-graphene layer floats on the surface, 6) graphene transfer to target substrate, 7) substrate is dried and, 8) the PMMA layer is removed.

In step 1 a silicon wafer is oxidized to prevent the copper that is sputtered in step 2 to diffuse into the silicon during step 3 where the graphene is grown on top of the copper. After this, in step 4, the wafer is coated with PMMA and then diced into smaller samples. In step 5 the copper is etched away with 15% Iron(III) Chloride solution in water and the silicon substrate drops to the bottom, while the PMMA-graphene layer floats on the surface. After three rinsing water baths, the second with 1% HCl to remove metallic residue, the PMMA-graphene layer floats in water (step 6) and the target substrate is submerged under it and slowly raised in such a way that the graphene sticks to the surface. In step 7 the substrate is dried and baked to remove residual water from the boundary and promote the adhesion of the graphene to the substrate. Finally in step 8 the PMMA layer is removed with acetone, leaving the graphene transferred on the substrate.

Due to the lubricating effect of the water the graphene does not stick to a surface when it is pulled out of the water next to the floating graphene. The solution to this issue is to catch a part of the floating graphene with the edge of the target substrate, so that it folds around this edge and then pull the substrate out of the water slowly to avoid a large accumulation of water on the boundary.

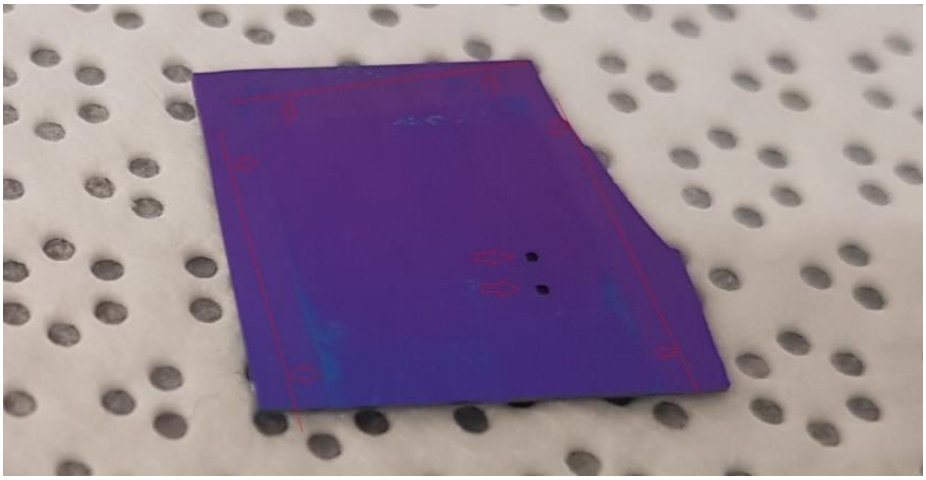

Figure 17. A sheet of graphene that is barely visible on a sample covering most of its surface (the edges are marked by red lines and arrows). The two membranes (marked by the two red arrows) that are covered by the graphene can easily be spotted as holes in the silicon substrate. These membranes stretch over an area of approximately 400x400 microns.

Another big issue in the transfer process was the adhesion of graphene to the membranes. Graphene is also considered to be a lubricant, so in general it does not adhere well to surfaces (Berman, Erdemir, & Sumant, 2014). The graphene only sticks to the surface due to Van der Waals forces so the adhesion is not that strong, something that is not helped by a high surface roughness or a curvature in the surface. However the surface roughness of the ALD alumina layer was less than 1.5 nm, which was measured with Atomic Force Microscopy (AFM), so this should not be a large issue. However the membranes themselves are wrinkled due to internal stresses, something that can be observed in figure 18.

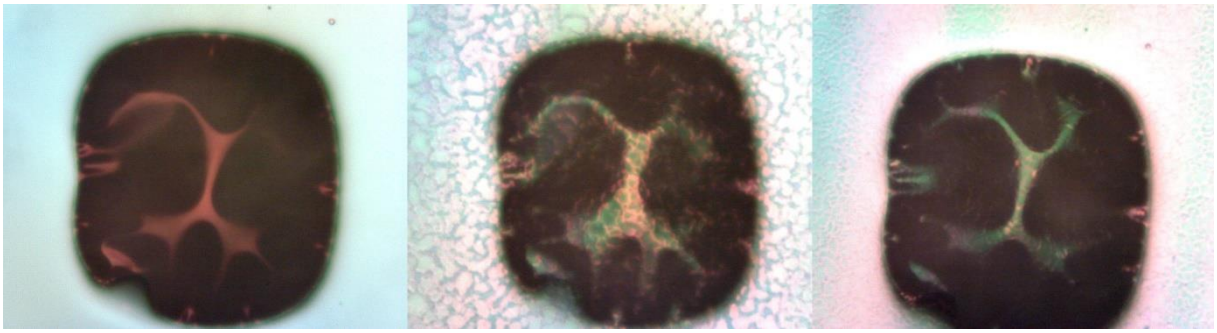

Figure 18. A membrane sample (a) before transfer, (b) after graphene transfer and (c) after a post-transfer bake to improve adhesion of the graphene to the membrane. The membranes shows signs of wrinkling, which does not favour the adhesion of the graphene layer.

Any residual water on the boundary would also negatively affect the adhesion, especially when the PMMA was removed with acetone after the transfer. During this step the graphene was washed of the surface of the sample along with the dissolving PMMA. In order to remove any remaining water on the interface and improve adhesion the sample was placed on a hotplate first at 70 ^{o}C and after 1 minute at 120 ^{o}C for 5 minutes to avoid gas forming and rapid expansion of gas, which could break the membranes. The effects of this treatment as seen under a microscope can be observed in figure 18. This procedure improved the adhesion, but the undesired removal of the graphene by the acetone remained an issue, which occurred 9 out of 10 times.

2.5. Results - Measuring Secondary Electron Yield

The membranes with the transferred graphene were tested in a Scanning Electron Microscope (SEM), specially equipped with a special sample holder, a Faraday cup, and three Keithley 2450 Sourcemeters to provide and measure current to the beam and to the sample and simultaneously measuring the transmission electrons. The measured currents are normalized with respect to the current of the e-beam and these are the electron yields presented. More information on the measurement method can be found in appendix B. The maximum yield is found by adjusting the energy of the primary electrons that are generated in the electron gun. For each electron energy that was selected a measurement is carried out and the data on the exact current is collected from the oscilloscopes. With this data graphs of electron yield versus electron energy can be produced, like the one in figure 19. The SEM creates images of surfaces by shooting electrons at the surface and collecting the backscattered electrons. Since different atoms have a different yield of backscattered electrons at a given energy of primary electrons, different materials can be distinguished. This helps in locating the membranes for the measurements and taking pictures of the membranes.

Graphene on Aluminium Oxide

All of the alumina membranes used for graphene transfer were 25 nm thick. This thickness was already determined to be ideal, because thinner membranes proved to be too fragile to handle during further process steps and thicker membranes had lower transmission yields and the primary electron energy were this yield was maximal was also too high to be practical. The SEM measurements of samples with graphene as a conductive layer will be directly compared to samples with TiN, in order to see if there are any advantages of using graphene. The expectation was that graphene would give the same yield profile as TiN only shifted slightly to lower energies, because electrons have to travel through less material, before reaching the emission side.

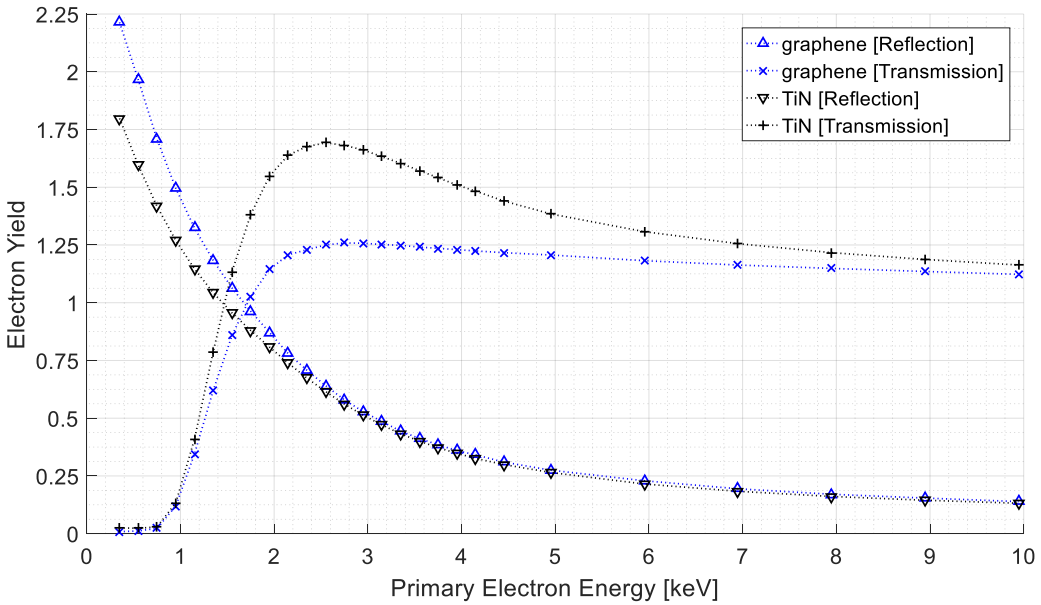

Figure 19. A direct comparison of the SEM measurements on total transmission and reflection yields of graphene and 5 nm thick sputtered TiN on membranes of 25 nm alumina. It can clearly be seen that the membrane coated with TiN gives a much higher transmission yield than the sample with graphene. The lower yield of the graphene sample indicates that the conductivity to the alumina layer is not good enough and charging effects are observed. The reflection yield of graphene is higher than TiN, but this is not of importance for this project since only the transmitted electrons will be multiplied in the detector. This does indicate that the graphene itself is conducting, but the connection between the alumina and graphene is not good enough to prevent charging effects in the alumina. The data points can be found in table 1 in Appendix B.

In figure 19 a SEM measurement of the transmission and reflection yield of a sample with titanium nitride and a sample with graphene as the conductive layer is compared. The transmission yield of the graphene sample is significantly lower than the TiN sample. This can be caused by poor adhesion between the graphene and alumina membrane. This would mean that during the measurement the graphene was not conducting enough electrons into the alumina membrane, which caused the alumina membrane to charge up locally. When this charging effect occurs, the transmission yield is suppressed to 1, something that can be observed in figure 19. However, the lower transmission yield can be partially contributed to the geometry of the sample. The membrane is created by etching a cavity in the supporting silicon substrate. When the conductive layer is applied this can be done on either side in the case of TiN, however the graphene cannot be placed on the side of the cavity as it cannot be stretched enough to cover the walls of the cavity, it will be suspended over it. This geometry, with the cavity facing the collecting electrode, negatively influences the transmission yield, since not all electrons are captured by the detector, but some will impact the edges of the cavity and will be absorbed into the silicon substrate (figure 20).

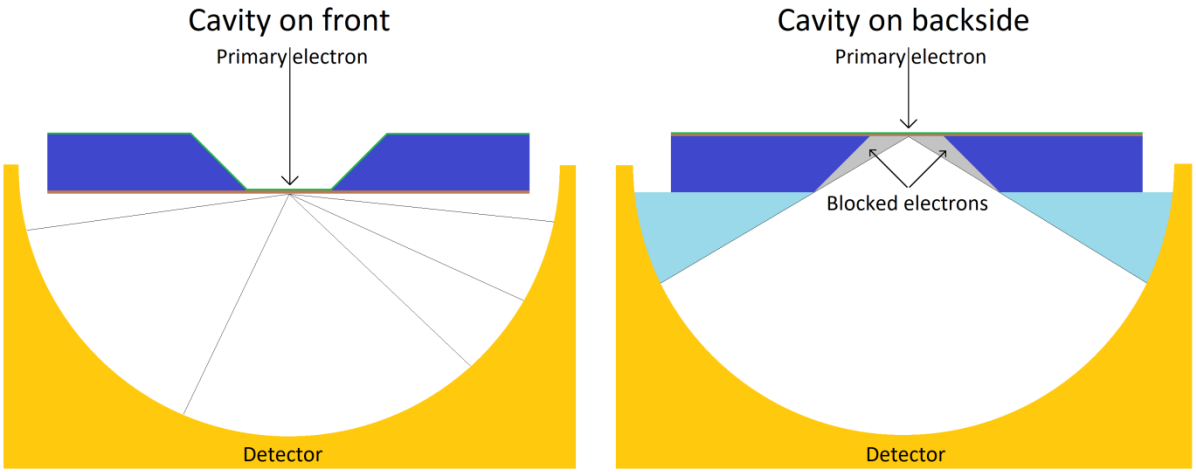

Figure 20. The geometry of the sample inside the SEM. When the conductive layer (and thus the cavity) is on the front side (as seen from the primary electron), all transmission electrons can get directly to the detector. However, when the cavity is on the backside certain angles of transmitted electron are obstructed by the cavity, resulting in a lower detected yield.

Another contributing factor to the low transmission yield might be the fact that a perfect sheet of graphene conducts electricity along its surface, but not through it. However the graphene that is produced for this experiment is not a perfect sheet, as it starts to grow from many places with many different crystal orientations. This means that our sheet of graphene consists of many ‘islands’ of graphene that come together in so called grain boundaries. On these grain boundaries the electrons have a small chance to scatter and even get to the other side of the graphene sheet (Zhang, Lee, Gong, Colombo, & Cho, 2014). However, the amount of resistivity of the graphene through the grain boundary to the other side of the sheet has not been extensively measured and no clear result regarding this could be found in literature. Since the current to the graphene layer is applied to the top side and drawn from the bottom side, this low conductivity through the sheet might be the cause of the low transmission yield combined with the poor adhesion of the graphene layer to the alumina.

Another important result that can be observed in figure 19 is that the electron energy, where the maximum transmission yield is observed, is not significantly different for the graphene sample compared to the TiN sample. This was not the expected result. As graphene is a monolayer the

chance of the primary electron to pass through this layer unhindered should be much higher than for the TiN layer where the electron has to pass many more atoms before getting to the alumina layer. However, this result shows that there is no difference in the primary electron energy where the maximum yield is found between these materials.

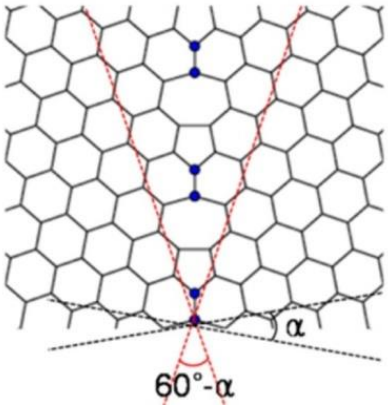

Under a microscope or in the SEM the graphene looks quite flaky, which is caused in the creation process, where the graphene starts to grow in multiple places at once forming small sheets (grains). This means that the resulting sheet has a polycrystalline structure and where the different grains meet grain boundaries are formed, where the crystalline structure is interrupted (figure 21). All of these separate grains form a kind of islands of graphene, which have worse adhesion to neighbouring grains and these grains can be removed during processing of the samples, resulting in the flaky appearance.

Figure 21. A grain boundary in graphene. Where the two grains meet irregular connections are made and the crystalline structure is interrupted.

In the area on and around the membrane the graphene seems to stick particularly worse to the alumina layer compared to the rest of the sample. As one can observe in figure 22 (and 23), the graphene is removed from the area around the membrane. This could mean that the adhesion around the membranes is worse than on the rest of the alumina layer, perhaps caused by buckling of the alumina membranes due to internal stresses after they are released from the substrate. The graphene layer sticks reasonably well to flat surfaces, but cannot follow curvatures that well. This would mean that the graphene was only in contact with the membrane in a few places.

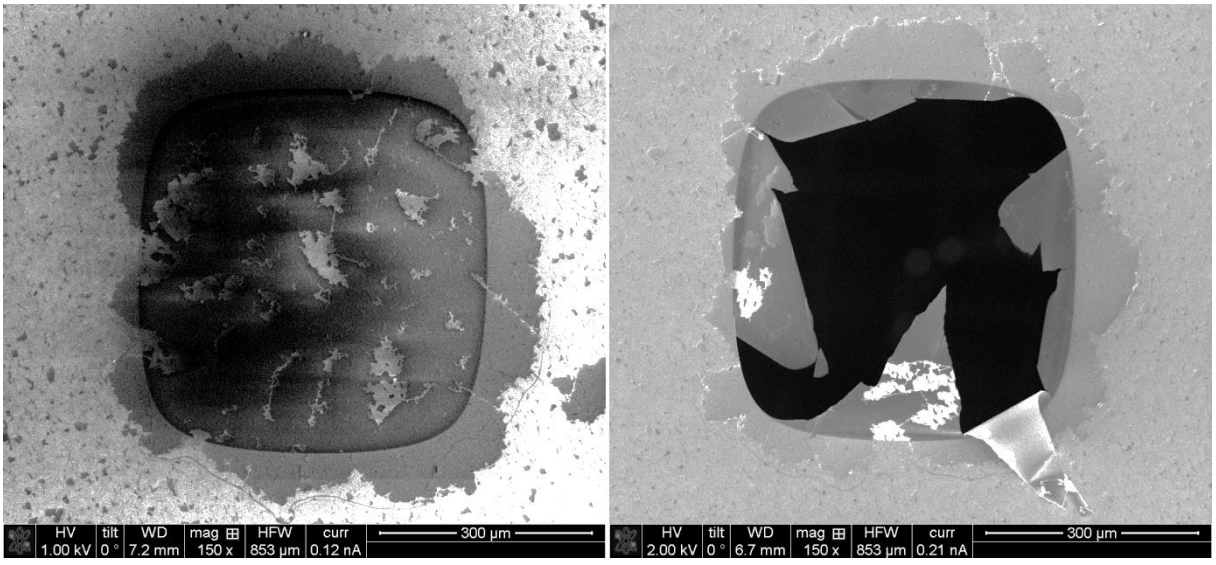

Figure 22. Two pictures of membranes made in the SEM. On both images can be seen that the graphene (relatively light coloured) is surrounding the membranes on all sides, but looks to be removed from the actual membranes. This is caused by the poor adhesion combined with movements of the membrane, possibly even by small vibrations due to sound waves. In the image on the right it can be observed that the presence of barely connected flakes graphene is sufficient to avoid charging of those parts of the membrane. This membrane was broken due to the force of liquid during transfer.

It can be seen in figure 23 that on the places where the graphene does stick to the membrane and is in contact with the main area of graphene on the sample, that the electric conductivity is good

enough to prevent the graphene on the membranes from charging up under the electron beam. The dark areas in the pictures do not produce as much reflection secondary electrons as the lighter areas, due to the fact that the area is charged up. The light areas do not show these charging effects and thereforee must be in electrical contact with the source.

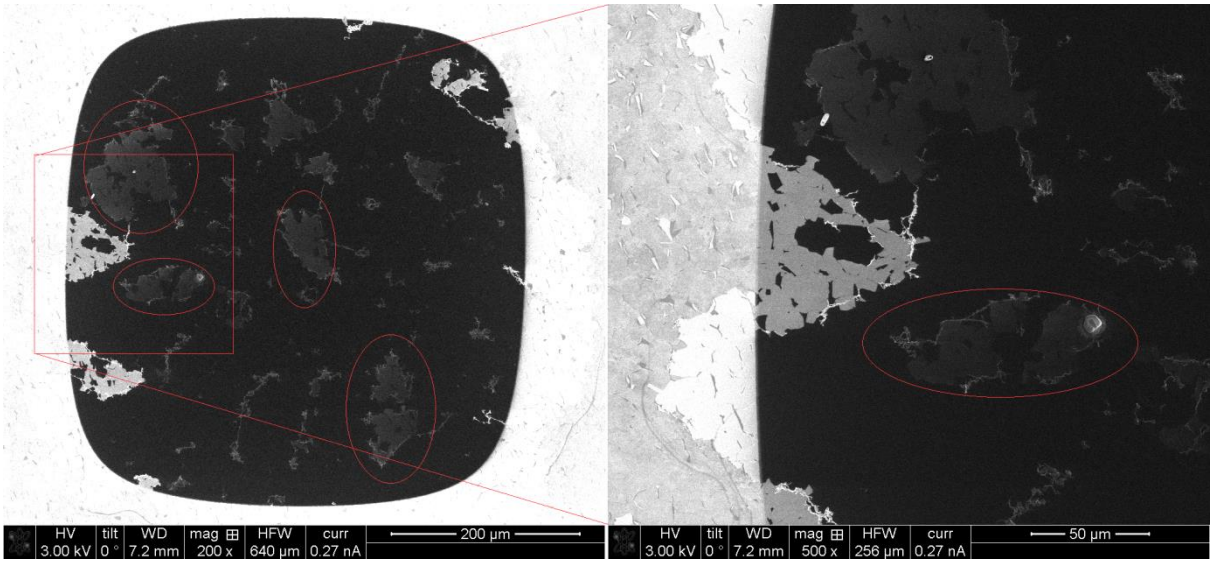

Figure 23. Two SEM images of the same membrane, the image on the right is a detail of the one on the left. On the left image several isolated islands of graphene (marked in circles) can be seen on the surface. As these islands are not connected to the graphene surrounding the membrane these areas charge up under the electron beam and become dark. In the image on the right a small patch of graphene on the membrane is actually connected and prevents the charging effects of the membrane in that area. This means that if the graphene is properly attached to the membrane it is sufficiently conductive to prevent any charging of the membranes.

The SEM images inm figure 22 and 23 show that there are large islands of graphene that are large than 30 micron in diameter. If one would be able to place such islands exactly over the membranes that are used in the TiPC design, which have a diameter of 30 micron, and achieve a good adhesion, the conductivity issue could be solved. The area between the membranes can be designed to conduct electricity and the graphene islands only need to make contact with this conductive area around the membranes. Placing these graphene islands with such precision may be currently very difficult, but future developments may make this possible.

Alumina Arrays

As can be observed in the impression of the final TiPC device in figure 3, the alumina membranes are designed in arrays that correspond with the underlying CMOS chip. Some tests were done to cover such arrays with graphene as well and these samples were checked in the SEM.

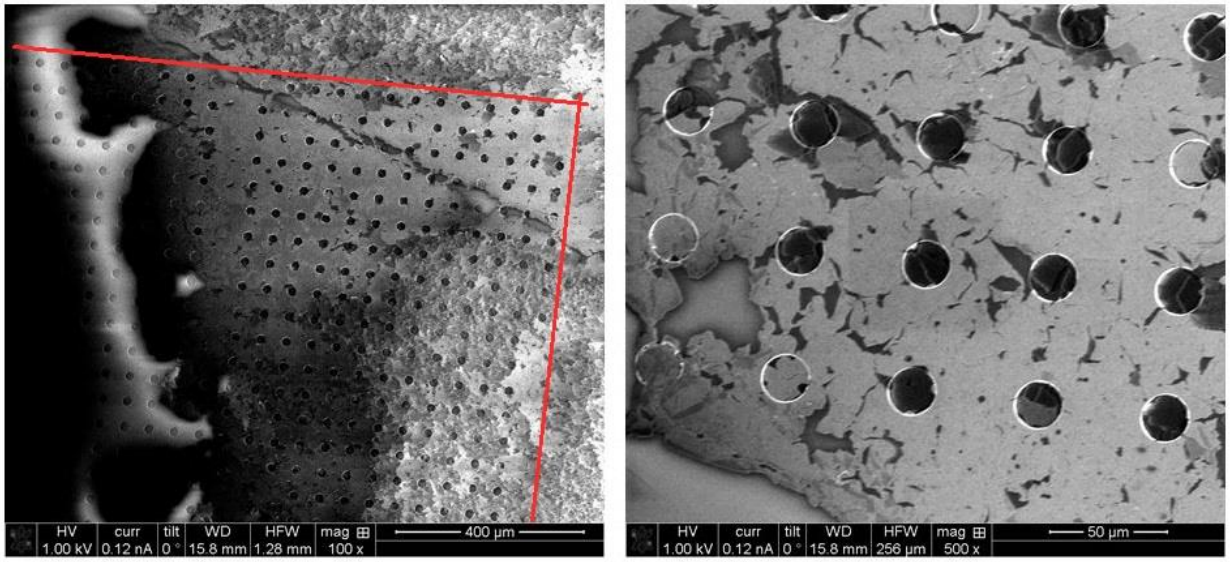

Figure 24. SEM images of the array covered by graphene. The borders of the array are highlighted in red. The image on the left shows that large areas of the array are showing charging effects and therefore reflect less electrons and thus appear dark in the image. Where the the graphene is conducting enough electrons to the membrane, the membranes in the array clearly show up as dark circles, indicating that the graphene has been washed away due to poor adhesion.

As can be observed in figure 24, the membranes in the array clearly show uop as dark circles. This means that the membranes are charging up and that the graphene that is covering the array has been washed away from most of the membranes. In the image on the right of figure 24, one can see that some membranes are covered by graphene. However, all of the covered membranes showed charging effect under prolonged exposure by the electron beam, making any secondary electron yield measurements on the samples impossible, as these require long measurements. The reason for this poor adhesion lay partly in the design of these arrays as can be observed in figure 25. The membranes lay embedded in the surface and the graphene could not fall into these indentations using the wet transfer method with PMMA.

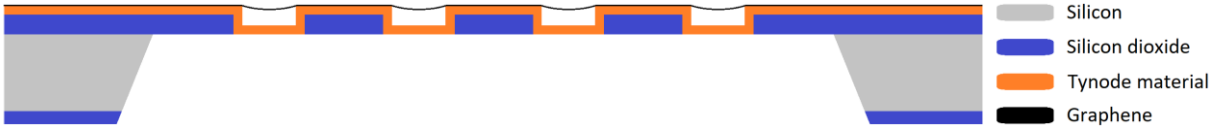

Figure 25. The array design involving many membranes, that lay embedded in the silicon dioxide layer, lead to even worse adhesion as the graphene could not follow the sharp indentations in the design. Since the graphene is not resting on the membranes of the array the graphene sheet will most likely be completely washed away during due PMMA removal. If the graphene did survive, it is not in contact with the membranes, so they would charge up.

The final design of these arrays will also involve curved membranes to have the desired focusing effect that can be seen in the simulations in figure 2. These bulges in the array would result in an even worse adhesion of the graphene as it would be suspended over the tops of the membranes instead of resting on the array as indicated in figure 26. This would mean that the graphene is even more likely to be washed away during the transfer and cleaning process. Since the the alumina arrays were not resulting in any measurements it was decided to not proceed with transferring graphene on

these samples, but focus on flat single membranes in order to proof the concept of using graphene as the conductive layer.

Figure 26. The final design of the tynodes involves bulging membranes to have the desired focusing effect. This would result in a similar issue where the graphene is suspended between the bulges. This would also result in the graphene being washed away during the PMMA removal with acetone.

In future research one could solve this issue by creating a graphene layer that bulges in the same way as the alumina membranes. This can be achieved by using the same method that is used to create the membranes, but instead of depositing alumina, copper would be sputtered. This should lead to a copper layer that bulges in the same way as the alumina and if graphene is grown on this layer, it is bulging in the same way. The problem that needs to be solved then is how to align the bulges in the graphene layer with the bulges in the alumina array, which should be investigated.

Graphene on Magnesium Oxide

Graphene was successfully transferred onto a magnesium oxide (MgO) membrane, where the adhesion issues appeared to be less profound. This could mean that the MgO samples are less buckled compared to the alumina samples or the graphene adhesion to MgO could be better than to alumina. Due to the very limited supply of these MgO samples, which have been coated with MgO in Argonne National Laboratory in the United States of America, only two samples were coated with graphene and one of these was successful. Images of this sample can be found in figure 27.

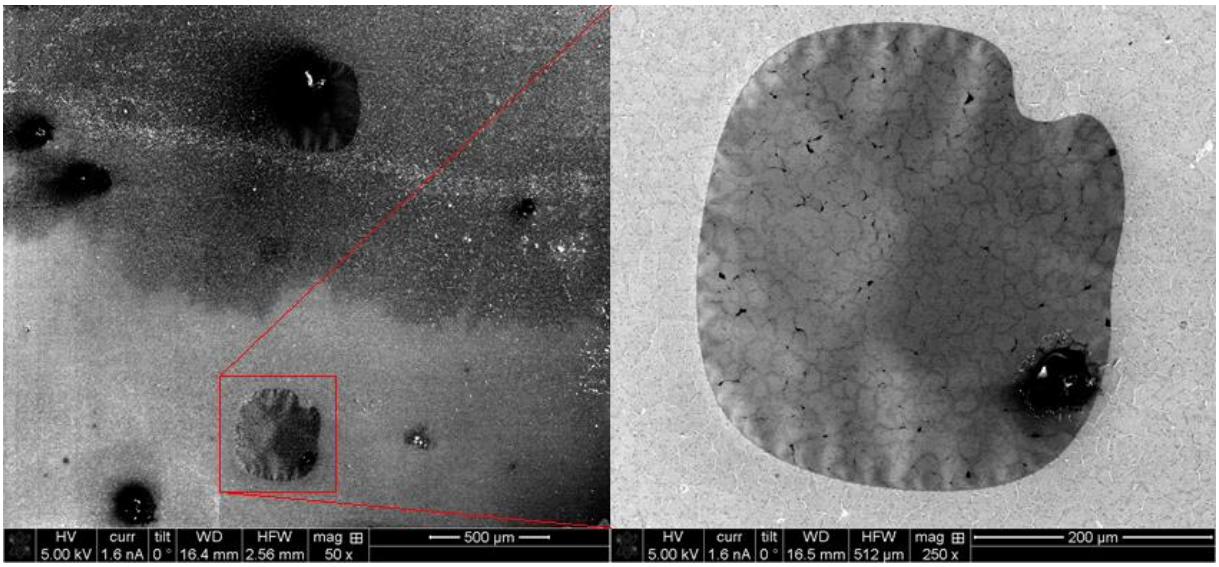

Figure 27. SEM images of an MgO sample covered with graphene. The image on the left shows two membranes, one in the top part and one in the bottom part of the image. The whole area is covered with graphene, but there is a clear divide between the top and bottom part of the image in terms of electron reflection. This might be caused by some residual PMMA on the top part. The membrane in this part of the image was thereforee deemed not to be suitable for measurements. There are also several holes in the graphene layer, this might be caused by imperfection in the graphene and might have been washed away with acetone while removing the PMMA layer. The image on the right is an enlargement of the bottom membrane of the image on the left. In this image the flaky structure of graphene is clearly visible and most of the membrane is covered. A small part of the membrane is not covered by the graphene (the black hole) and the membrane is not fully released from the substrate, this can be easily spotted in the upper right corner.

Since the MgO samples were much more fragile than the alumina membranes and could possibly dissolve in water, the time that the membranes were in contact with any fluids during the transfer of graphene was limited to a minimum. This also meant that the time the membrane was held in acetone was minimal, less than one minute, compared to four or 5 minutes for alumina membranes. This means some residual PMMA was left on the sample, which caused the difference in reflection yield image in the SEM (and thus the image brightness) between the top and bottom of the left image in figure 27. The indentation of the membrane that can be seen in the right image in figure 27, which is very different from the normal geometry like the one in figure 23, is most likely due to an incomplete removal of the silicon dioxide from the back of the membrane. This incomplete release of the membrane can also explain the much lower transmission yield of the sample compared to previous MgO samples that were coated with TiN. The result of the measurements in the SEM of this graphene-MgO sample in direct comparison with the TiN-MgO sample can be found in figure 28.

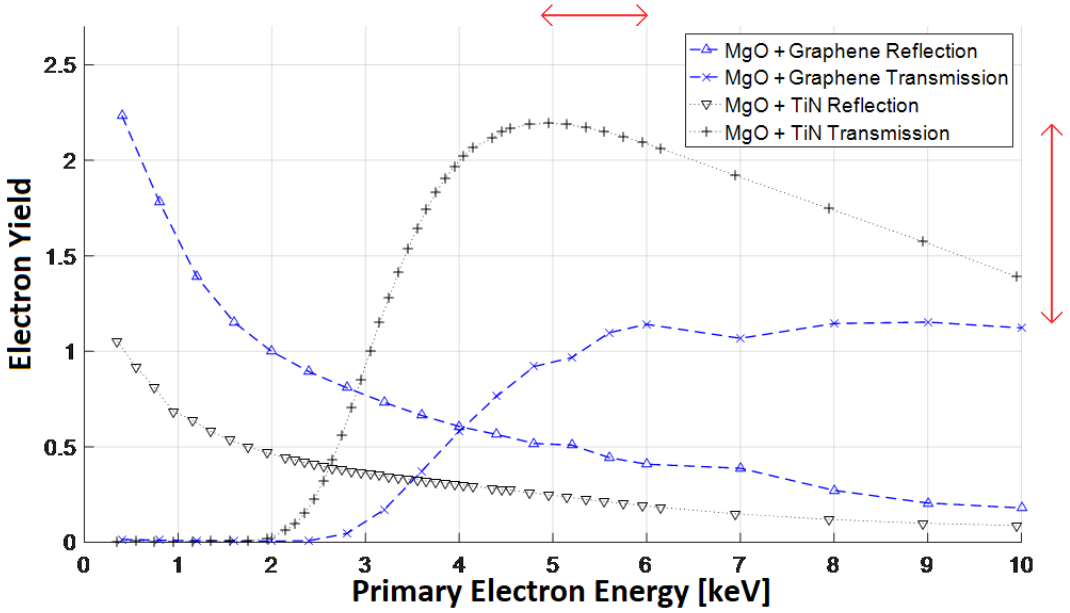

Figure 28. Results of SEM measurements on the MgO and graphene membrane compared with another MgO sample coated with 5 nm sputtered TiN. From these measurements can be clearly seen that the transmission yield of the sample with graphene is much lower than the sample with TiN. The peak transmission yield of the graphene sample is found and a significantly higher primary electron energy 6 keV compared to 4,9 keV and the energy where the first transmission electron appear is also higher, 2,5 keV compared to 2 keV of the TiN sample. This could be an indication that there was still a thin layer of silicon dioxide on the backside of the membrane, which was thereforee not fully released. This oxide layer would block transmission electrons until the primary electron energy is sufficient to pass into this layer and create secondary electrons. The yield of silicon dioxide is comparable with the yield found in this measurement. The data points of this figure can be fgound in Appendix B table 2.

The reflection yield of the graphene sample is much higher than the reflection yield of the TiN sample. This proves that the conductivity in the graphene layer is good and that the connection to the electron source outside the setup is also good. Just like the results from the alumina sample, the transmission yield does not rise far above 1, indicating charge up effects in the alumina layer. This would mean that the conductivity from the graphene layer to the MgO layer is not ideal, most likely due to adhesion issues. This could mean that there are not enough points of contact between the graphene and the membrane. Besides the lower transmission yield also the energy where the first electrons pass through the graphene sample is higher than the TiN sample and the maximum transmission yield is observed at a higher primary electron energy. This is contrary to the expectation

that this energy would be lower than that of TiN samples, because of the single layer of carbon atoms the electrons should pass compared to many atoms in TiN. The combined effect of a low transmission yield and a higher primary electron energy where the maximum is observed can also indicate that the membrane was not properly released and a thin silicon oxide layer still resided on the backside of the membrane. An oxide layer would make the membranes thicker and thereforee the electron needs more energy to pass through it and the secondary yield of silicon oxide is also comparable to the low numbers that are observed in this measurement.

2.6. Conclusion

Due to the many issues with the production of graphene, the transfer and the poor adhesion to the membranes, it is not advisable to use transferred graphene as the conductive layer in this device. The results that were measured in the SEM indicate that the primary electron energy, where the maximum yield is found, is higher for graphene samples than for TiN samples. Also the transmission yield of samples coated with graphene is actually lower than TiN samples, while the reflection yield is much higher. This means that the conductivity in the graphene sheet is actually good, but that the conductivity from the graphene layer into the membrane is not high enough to prevent charging effects in the membranes. The charging effect can be observed from the SEM measurement results, where the transmission yield is suppressed to 1. This lack of vertical conductivity from the graphene into the membrane is most likely caused by poor adhesion and few points of contact between both layers, but also the poor conductivity through the graphene sheet. The reasons for the failure of the method used in this research were firstly that the ALD alumina process was terminated with wrong precursor (H_2O instead of TMA) as a TMA terminated process fovours graphene adhesion. Secondly, graphene is actually a lubricant so it does not adhere well to any surfaces. Thirdly, the membranes were bulging due to internal stresses and the flat graphene/PMMA layer does not follow these curves very well. This last issue is also problematic when graphene is applied on the final design of the tynodes, where the membranes are placed in an array and are curved to have a focussing effect. A solution to this issue is to create a graphene layer that is shaped in the same way as the membranes and have the exact same pitch as the array.

This leads to the conclusion that transferring graphene onto these thin membranes is not a viable option using the methods that are used in this research. The SEM results show that the graphene samples have a low transmission electron yield, indicating a poor adhesion between the membranes and the graphene layer. Using the method described in this thesis, graphene is not suitable to replace TiN as the conductive layer for the tynodes. There might be a way to circumvent the adhesion and conductivity issues by depositing the alumina on the graphene through ALD, instead of transferring the graphene on the alumina. This is what has been tried in the final stage of this research and is described in chapter 4 of this thesis.

2.7. Discussion

Graphene Deposition Issues

Unfortunately it proved to be quite difficult to produce graphene of sufficiently good quality to be suitable for transfer. After a first test run, that proved successful in terms of quality and transfer possibilities, the CVD machine did not seem to be capable of producing a high quality monolayer graphene anymore. Many (over 60) tests with small pieces of copper were carried out, but Raman spectroscopy proved each of them to be either amorphous carbon or graphite. Since I was the only

user to grow monolayers graphene on copper and other users did not have the same issue on different substrates, like molybdenum, it proved difficult to pinpoint the exact cause of the problem. After several months the culprit was found to be a faulty Mass Flow Controller (MFC) for the methane supply that did not shut off completely. This meant that even when the computer would signal the MFC to let 0% flow, it still had a flow of more than 10%. This meant there was always a flow of methane in the reactor, while the machine was operating, even at lower temperatures. This lead to the deposition of too much (amorphous) carbon, which could not be used for transfer. After the MFC was replaced by a new one, all issues were fixed and high quality graphene was produced immediately.

Graphene Transfer Issues

There are several issues regarding the transfer process that became apparent during the course of this thesis. During the first test runs to transfer graphene from its original substrate to, in that case, a silicon dioxide sample, the graphene would not lift of its substrate after the copper layer was removed. This was due to the inferior quality of the graphene layer. The graphene layer would stick to the silicon substrate, making it necessary to use tweezers to remove it, destroying the sample in most cases. This problem was solved by using samples where the graphene was of good quality. With these samples the graphene-PMMA layer detached properly from the silicon substrate.

Graphene Adhesion Issues

The adhesion of the graphene layer to the substrates coated with alumina was less than ideal and the graphene was washed away while trying to remove the PMMA layer from the sample using acetone. Examples of this graphene removal can be found in figure 29. This was most likely due to some residual water on the boundary between the graphene and the substrate, preventing the graphene to have many Van der Waals bonds. When acetone was used to dissolve the supporting PMMA layer, it would remove the graphene as well or the graphene would fold up on itself as can be observed in figure 29 on the right.

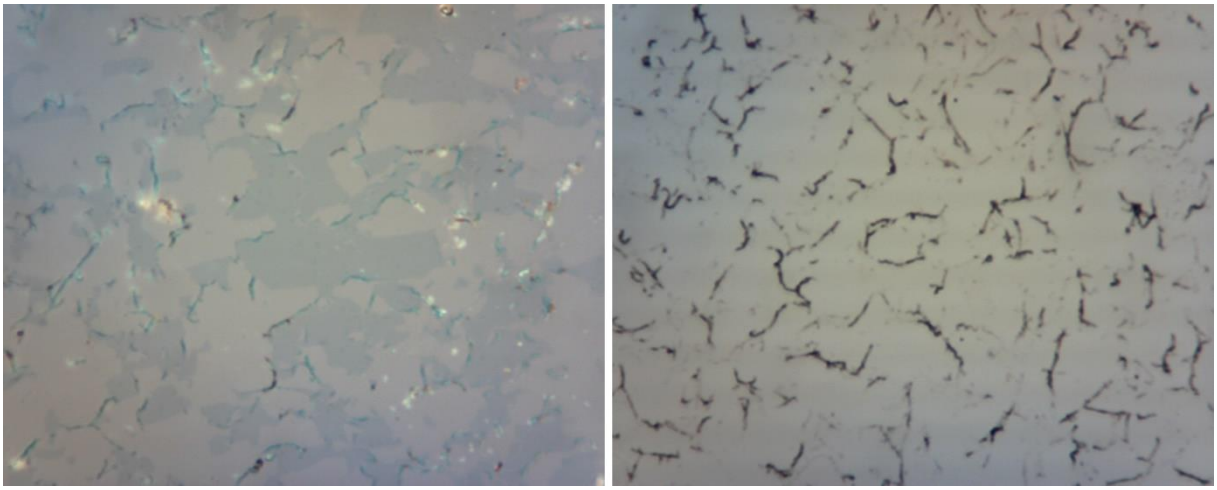

Figure 29. Microscope pictures taken of samples after the removal of the PMMA layer by acetone. On the left the darker patches are areas where there is still graphene left on the sample, but the lighter areas are stripped from graphene during the acetone step. In the picture on the right the graphene has partially released and curled up on itself, creating the thin dark strips of many layers graphene.

Several techniques were tried to improve the adhesion. After the transfer of the graphene-PMMA layer the samples were placed on a hotplate, in order to remove the residual water from the boundary between the graphene and alumina. The first samples were immediately put on a hotplate

that had a temperature of 120 ^{o}C, but the sudden expansion of gasses on the boundary destroyed some of the membranes. After this the samples were initially put on a hotplate at 60 ^{o}C for one minute until the boundary had visibly dried and then the temperature was increased to 120 ^{o}C and left for another 5 minutes to dry even further. Any higher temperatures would make the PMMA layer harder to remove, because it would be baked further than its initial softbake earlier in the process. This method improved the adhesion somewhat, but the issue of removing the graphene with acetone remained a problem. Also some tests were performed by placing samples in a vacuum oven at 200 ^{o}C where the air was continuously removed via a pump to create a pressure of 0.3 mbar. The samples were placed in this oven for two hours in order to remove the residual water from the samples. However, after this treatment the graphene was still washed away by the acetone, so this did not affect the adhesion any better than the hotplate method.

The time that the samples were put in the acetone was also reduced from 5 minutes to shorter periods, but this left PMMA residue on the samples, so this was not a viable option. Furthermore, the temperature of the acetone was increased to 45 ^{o}C, any higher would evaporate the acetone too quickly as its boiling point is at 56 ^{o}C. This meant the PMMA was removed quicker and the samples could spend less time in the acetone, but this did not seem to positively affect the graphene removal. To increase the effectiveness of the acetone, an ultra-sonic bath was proposed. This only had negative results as most of the membranes broke due to the vibrations in the water. The graphene was also removed by this bath, so this was not a viable option. Also other chemicals were used to remove the PMMA layer, like N-methyl-2-pyrrolidone (NMP), but the same results were observed as with acetone. During the final weeks of the project critical point evaporation was proposed, that could be done in the Kavli cleanroom. However I missed the appropriate training to use chemicals in that cleanroom and there was not enough time anymore to get this training, so this technique was left unexplored.

At the end of the project some literature was found regarding graphene on ALD alumina (D.-W. Park, Mikael, Chang, Gong, & Ma, 2015). The research described in that paper shows that the terminating step of the ALD process is important to the adhesion to the surface. If the ALD process was terminated with the tri-methyl aluminium (TMA) the adhesion would be improved compared to a H_2O terminated ALD process. Unfortunately all the samples that were provided for this research were all terminated with the H_2O step of the ALD process, meaning that the graphene adhesion was less than ideal.

3. Titanium Nitride

Titanium Nitride (TiN) is the material that is currently used by the team to create the conductive layer on the membranes. The layer is deposited on the samples by sputtering, however in this chapter the possibility to use Atomic Layer Deposition (ALD) instead will be investigated. This technique was used in the final weeks of the research and only samples created for another project were tested, so the results are very limited.

3.1. Physical Properties TiN

Titanium Nitride is a high crystalline ceramic material and it has a body-centered cubic structure. It is an extremely hard material, which is why it is often used as a coating for drill bits. It can be easily regognized by its gold like appearance when this coating has been applied. In the semiconductor industry thin films of TiN are used as conductive layer, while also acting as barrier for diffusion of metals into the silicon. In the industry it is known as a "barrier metal" even though it is a ceramic material. This classification is understandable as TiN has an electrical resistivity of $4 \cdot 10^{-6}\ \Omega\mathrm{m}$ (Lengauer et al., 1995), which is close to most metals that have a resistivity between $10^{-6}\ \Omega\mathrm{m}$ and $10^{-8}\ \Omega\mathrm{m}$. This low resistivity (or high conductivity) combined with the ease of application makes TiN an ideal candidate for the conductive layer on the membranes.

3.2. Application Method

Sputtering

The current technique to deposit a conductive layer on the membranes is by sputtering titanium nitride (TiN) on them. Sputtering is a technique where electrons or ions are accelerated in 'vacuum' towards a solid surface, in this case titanium, where they dislodge atoms. These atoms get deposited on the surface of the sample, together with atoms from the low pressure nitrogen environment (so called reactive sputtering), thus creating a thin layer of TiN.

Atomic Layer Deposition

Atomic Layer Deposition (ALD) is a different technique to get a thin layer of TiN onto the sample. In this technique the sample is placed in a reactor where a vacuum and a temperature of 250^{o}C is applied. Then the two precursors are alternatingly introduced in the reactor in cycles, where the number of cycles correlates with the thickness of the TiN layer. The precursors used in this process are Titanium chloride ($TiCl_4$) and nitrogen plasma, which under the applied circumstances will adhere to the surface and start building up a thin layer of TiN. Since each precursor step is self-limiting, this process can be controlled very accurately and thereforee the thickness of the deposited layer can be controlled on a atomic layer or Angstrom level.

3.3. Results

First the recipe that was available for this deposition process was tested on samples coated with alumina, in order to see whether this deposition would work. The deposition rate of this recipe should be around 1.7 Angstrom per cycle, based on prior depositions performed by this machine with the same recipe. Therfore 30 cycles were chosen and performed at 250 ^{o}C, which should result in a layer of 5 nm. An in situ ellipsometer was installed in the machine, making it possible to measure the layer while it was deposited. A graph of this measurement performed during the deposition of TiN on alumina can be seen in figure 30.

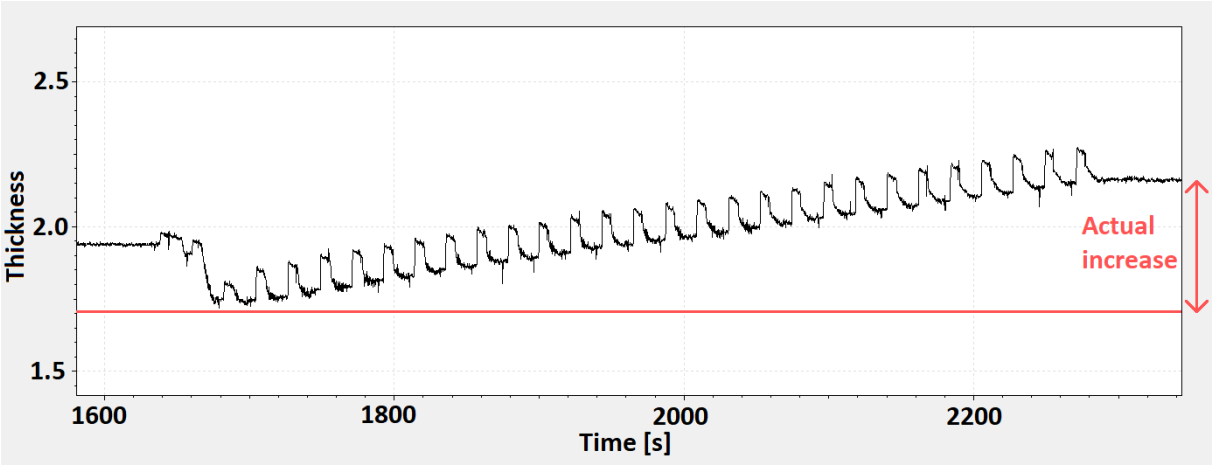

Figure 30.The measurement of a TiN deposition on alumina by the in situ ellipsometer. Some strange effect can be observed at the start of the deposition, where the initial thickness of the sample appears to go down, before the layers are added. To compensate for this, the red line is added to indicate the lowest measured point and the actual increase in thickness.

In figure 30 the intial thickness of the sample appears to go down at the start of the deposition. This has to do with the way the ellipsometer performs its measurement, the sample does not actually decrease in thickness. A beam of light is filtered through a polarizer before it is send to the sample under a specific angle, in this case 30°. The refelected light is less polarized than the inbound light and this change in polarization is measured and helps determine the thickness of the layer. This change in polarization is material specific and thereforee the material needs to be selected. The alumina sample has a change in polarization that corresponds to a thicker layer of TiN, so when the TiN is initially deposited, the ellipsometer measures a change in polarization that is different from the initial layer and the thickness of the sample now appears smaller. The measurement quite clearly shows that TiN is deposited very well on alumina samples. Thereforee some samples were created for a different project, that were tested in the same set-up in the SEM as used the other measurements in this thesis. However, these results themselves are not part of this thesis, but they are only used to indicate the effectiveness of TiN deposited by ALD as conductive layer. Figure 31 contains a drawing of how these samples are build up.

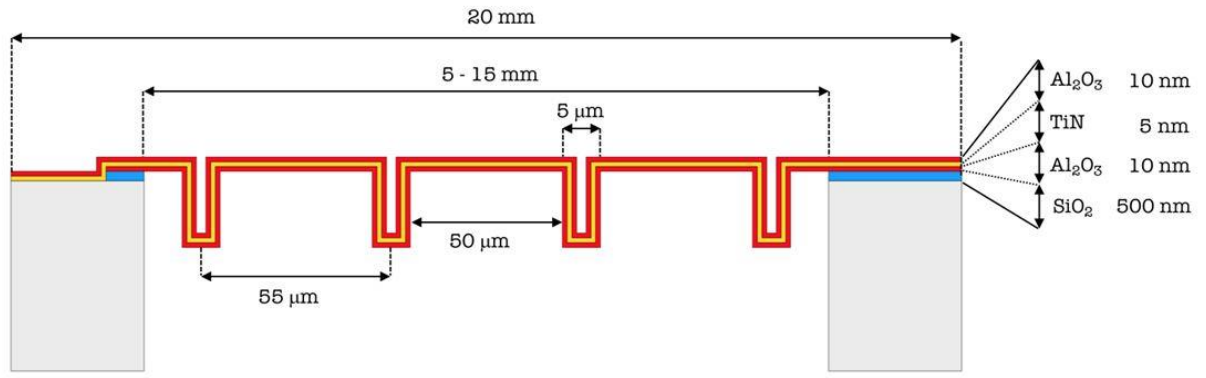

Figure 31. A schematic drawing of the samples used in the other project. The TiN and top alumina layer were deposited by me in the ALD at Kavli. (Chan & Graaf, not published)

The results from the tests performed on these samples can be found in figure 32.

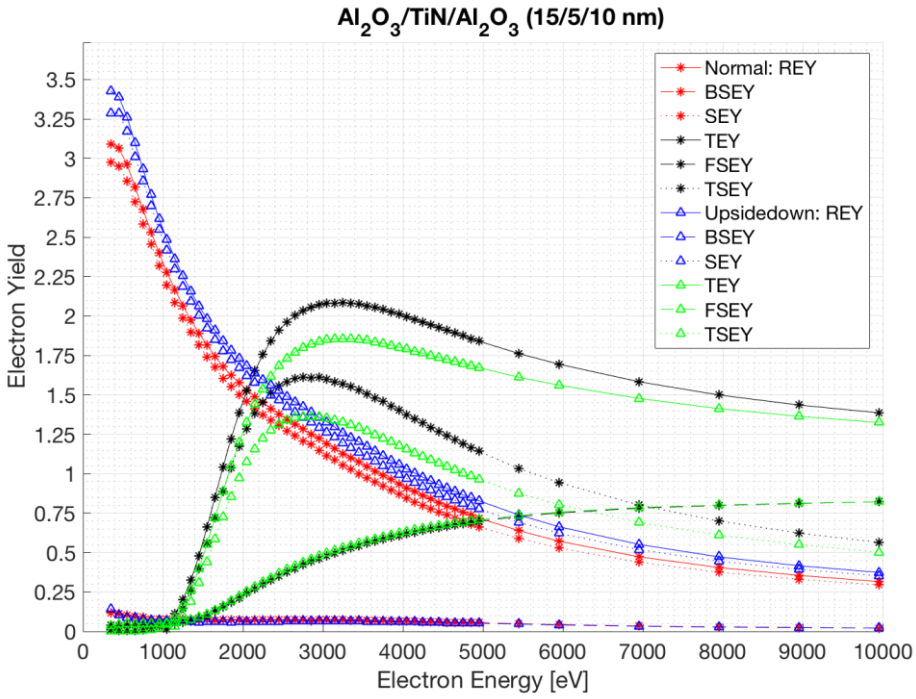

Figure 32. The results from tests performed on the samples containing ALD TiN. There are no signs of any charging effects in these samples, the transmission yields are significantly higher than 1. This means that ALD TiN is working well as the conductive layer in the membrane. The difference between normal and upside down is the placement of the sample as described in figure 20. The emitted electron collide with the cavity walls and are therefore not measured. (Chan & Graaf, not published)

The results from this measurement show that the 5 nm ALD TiN layer is conductive enough to prevent charging effects in the membrane. This proves that ALD is a good method to replace sputtering to deposit the TiN.

3.4. Conclusion

TiN deposited by ALD works well as the conductive layer in the membranes used for this project. This means that all layers of the membrane can be created in a single session in the ALD reactor, saving time in the production process. An important improvement that can be researched in the future is the decrease of thickness of this TiN layer. Currently 5 nm was chosen in these samples to prove the concept, but more research is needed to find the minimum thickness of the layer, where it still conducts enough electrons to prevent charging effects in the membrane. A thinner conductive layer should increase the transmission yield and lower the primary electron energy at the maximum yield.

4. Transfer-free Graphene-Alumina Membranes

In order to circumvent the adhesion issues of graphene to the alumina membranes, another technique was explored where alumina was deposited directly on the graphene through an ALD process. Using this process a new procedure to create tynodes could be developed that does not include a transfer step. Thereforee this procedure circumvents most of the adhesion problems as well as not having to deal with the removal of PMMA that was needed for the transfer of graphene.

4.1. Alumina ALD on Graphene

One of the essential steps in creating a membrane in this way is the deposition of alumina on the graphene layer in the ALD reactor. This can be problematic since perfect graphene does not have any nucleation spots where the ALD process can start from. The solution is to do a treatment of the graphene prior to the ALD process in order to create seeds on the graphene that can act as these nucleation spots. There are several methods to achieve this among which are a H_2-plasma treatment combined with an 400 ^{o}C anneal after the ALD process (Vervuurt, Karasulu, Verheijen, Kessels, & Bol, 2017), a NO_2/TMA treatment before ALD (Wang et al., 2012), a TMA/H_2O treatment (Y. H. Park et al., 2016) and H_2O treatment of the graphene (Zheng et al., 2014). After investigating these options the choice was made to perform the TMA/H_2O treatment, as this could be performed in the ALD reactor available for this project and did not need any extra process steps. With this technique the process starts with 5 cycles at 100^{o}C of a TMA pulse and a 5 second period followed by a H_2O pulse with no purging of the gasses between these pulses, after another 5 second period the reactor was purged, ending one cycle. After 5 of these cycles the graphene pretreatment was done and the normal ALD cycles were performed to achieve the desired thickness. The normal cycles consist of the same method as the pre-treatment, but with an additional purging step between the TMA and H_2O pulse. This method proved to be successful and was also performed in a second ALD reactor with an in situ ellipsometer. The measurements of that ellipsometer can be found in figure 33. The cycles and increasing thickness of the layer can be readily observed.

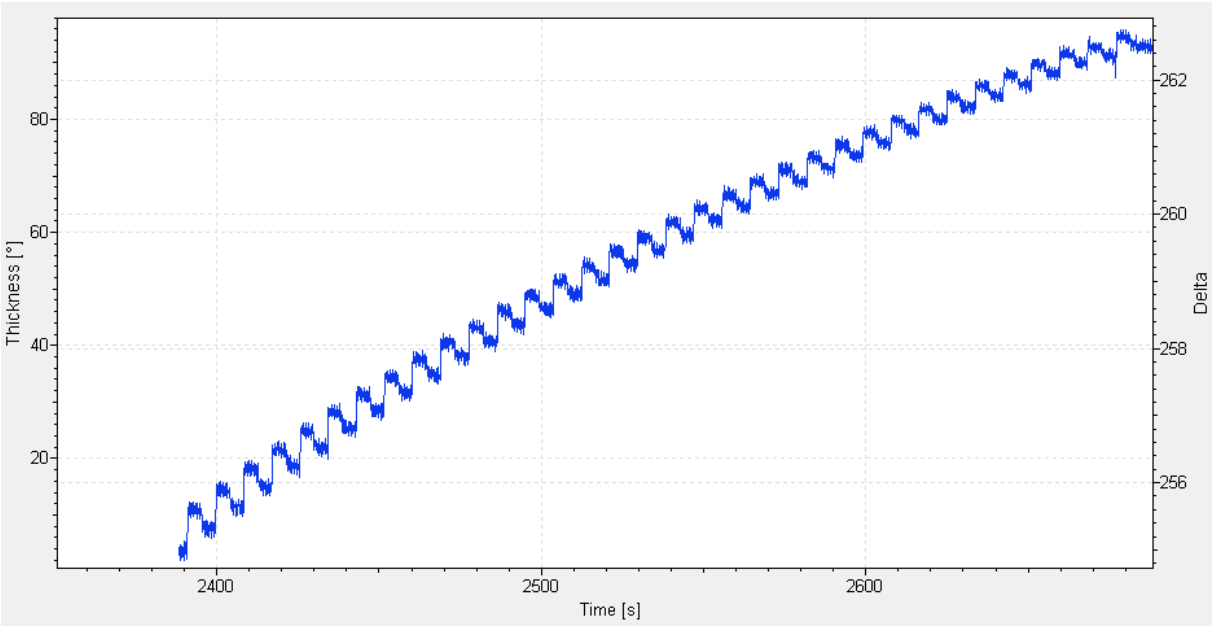

Figure 33. The measurements of an in situ ellipsometer in an ALD reactor where alumina is deposited on a graphene layer (300 cycles at 250 ^{o}C, only a part is shown). However the curvature in the graph hints to an inaccuracy in the ellipsometer, because the thickness should increase constantly for each cycle.

4.2. Process Steps

Since the deposition of alumina on a sheet of graphene was indeed possible, a flowchart was developed in which the complete process of creating membranes without graphene transfer is described. This flowchart is given in figure 34.

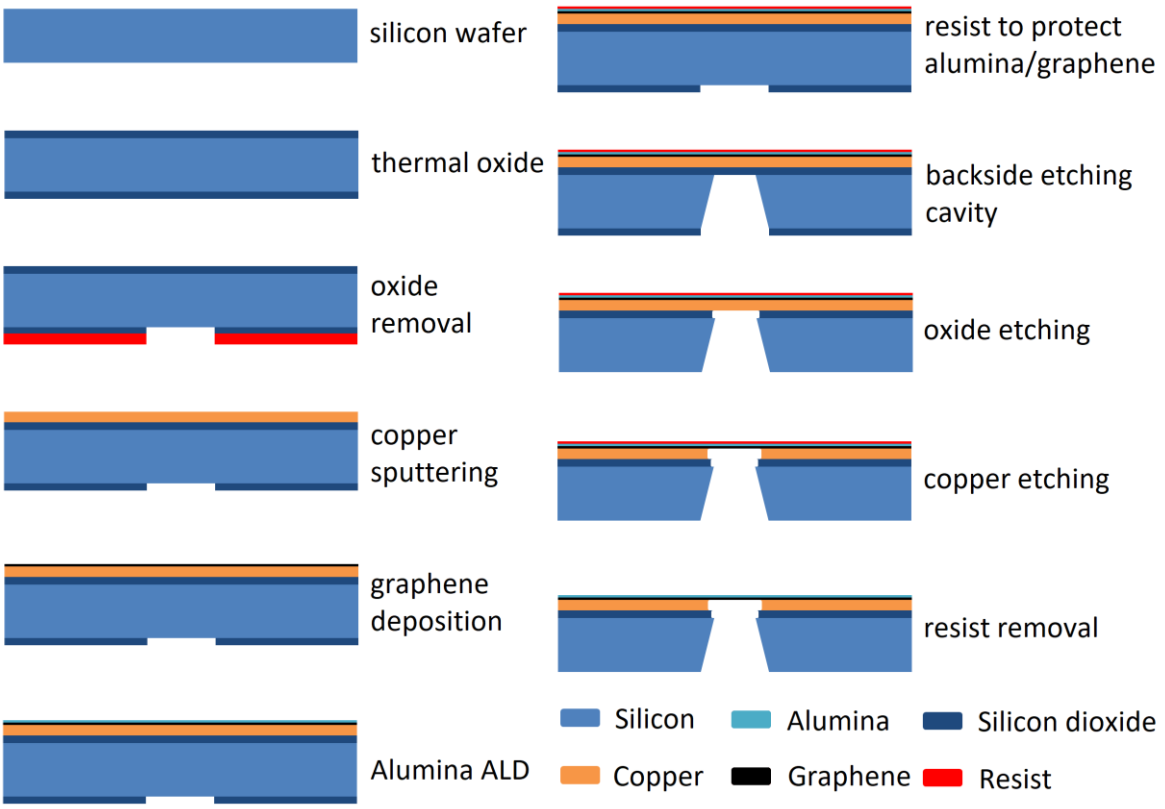

Figure 34. The flowchart for creating the alumina-graphene membranes without the need to transfer the graphene onto the alumina.

The membrane was created in a specific order, to take into account that some chemicals used in one step can remove a layer that was deposited earlier. Also some steps need to take place before another can be performed. First a 200 nm layer of silicon oxide was grown on the 300 micron thick silicon wafer to prevent the copper from diffusing into the silicon during the graphene deposition, which takes place at around 900^{o}C. This oxide layer is also used on the backside as a stopping layer for tetramethylammonium hydroxide (TMAOH), which is used to make the cavity in the silicon in order to release the membrane. Thereforee part of the oxide on the backside of the wafer is removed by plasma etching after placing resist over the areas that need to stay. This resist is then removed and the wafer is cleaned.

The ideal next step would be to create the cavity in the silicon, however the silicon oxide layer might be too weak to be self-supporting due to large stresses in the layer. As a precaution, graphene and alumina layers were deposited first (in the same way as described earlier) and to protect these layers resist was applied as well. The cavity was created using TMAOH 25% weight solution in H_2O at 85 ^{o}C in a specialized holder that protects the layers on the front side of the wafer. This solution should etch more than 0.6 micron per minute according to literature (Steinsland, Finstad, & Hanneborg, 2000), so the 300 micron silicon layer should be etched in 500 minutes. After the cavity in the silicon

was created, the oxide layer (200 nm) from the backside and inside the cavity was removed with HF vapour etching for 4 minutes (50 nm per minute). After this step the copper could be etched away through the cavity as well, releasing the alumina-graphene membranes. The final step was to remove the protective layer of resist that was deposited on the front.

4.3. Difficulties

The choice to use copper so early in the process proved to be problematic, because within EKL this is a so called 'red' metal. This means that it easily contaminates chemical baths and can cause problems in other people's devices. This is caused by the fact that copper can be so easily absorbed in silicon and ruin any P-N-junctions that are being created. Because of this, new chemical baths had to be created for this purpose with the limited available lab equipment that could be used for contaminated solutions. This meant that the temperature could not be controlled as precisely as desired. A solution to this might be to increase the thickness of the oxide layer to make it stronger and to etch the silicon before the copper was applied.

It was decided to use five wafers to do this run and every wafer contained 37 membranes that could be diced into separate samples through dicing lines that were etched away simultaneously with the cavities. This would have yielded more than enough samples to test the membranes, but due to the fact that the thin wafers were fragile and the many process steps, only a single wafer survived the silicon etching. The pattern used to create dicing lines into the silicon was the reason that the samples were so fragile. This created square samples by etching a grid into the wafer. The silicon was etched over the full length and width of the wafer, removing most of its strength (see figure 35).

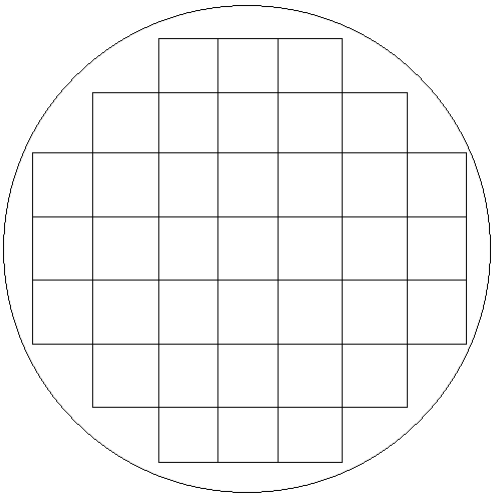

Figure 35. The grid etched into the silicon, which made the wafers very fragile during processing.

Creating a pattern that would not incorporate dicing lines that run almost over the full length of the wafer would help to circumvent this problem. Another solution would be to etch the dicing lines less deep, preserving a thicker layer of silicon and thereforee more strength in the wafer.

After the process of making the cavities, the oxide layer was etched away in the HF-etcher, again 10 minutes to etch 500 nm of thermal silicon oxide. Figure 36 shows a picture taken through a microscope of the membrane. This picture is taken from the backside of the sample, through the cavity that is etched in the silicon. At this point the copper

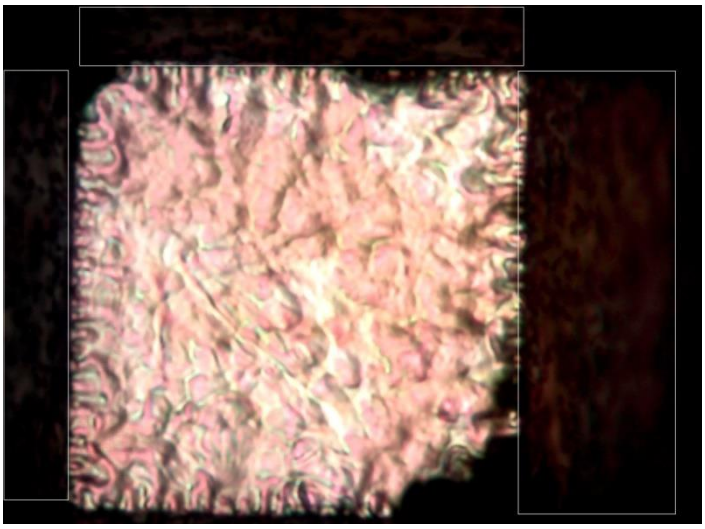

Figure 36. A picture taken through a microscope of a copper-graphene-alumina membrane, taken from the back side. The edges of the cavity can be distinguished (boxes in the picture).

could be etched away in order to release the alumina/graphene membranes. This proved to be avery challenging step since it was much slower than expected, more than half an hour instead of one minute and when the copper was removed several membranes broke. This process was tried on several samples, where on multiple occasions the complete copper layer was etched away, rendering the sample useless, since the graphene-alumina layer rested on the copper. The issue in this step might be that the oxide layer was not etched away fully by the HF vapour. This would have been a simple fix, by placing the samples in the HF etcher again, but the available cleanroom time for this project was fully spend by the time this solution was proposed.

4.4. Conclusion

No working samples of the membranes were produced, so there is no certainty to say whether this technique is viable to produce graphene-alumina membranes. If the steps of the process were all completed correctly, mainly the HF vapour etching of the silicon dioxide layer, working samples could have been produced with this technique, but the time limit for this research was reached. Thereforee this process could be tried in future research.

I would personally like to put the silicon etching step much earlier, directly after the third step where the oxide is removed from the backside. This would avoid the cleanroom restrictions on which devices and materials can be used, since the copper would be applied in a later step. Also a 200 nm oxide layer should be strong enough to stay intact, but the choice could be made to create a thicker oxide layer.

5. Conclusion

The transfer of graphene on alumina membranes in order to create a conductive layer appeared to be unsuccessful using the current method. The adhesion of the graphene to the alumina was in many cases not good enough to survive the removal by acetone of the PMMA layer used in the transfer process. In some of the cases where the graphene did stay attached through this process it was removed from the area where the membranes was located, most likely due to strong curvature of the membranes. The few samples where graphene did adhere to the surface of the membrane throughout the whole process were tested in a SEM equipped with a Faraday cup. This allowed for the simultaneous measurement of reflection and transmission electron yields. The results showed that the transmission yield, which is the important quality of a tynode, was lower than samples coated with TiN, the material currently used as conductive layer. Also the expected shift of the maximum yield to a lower primary electron energy was not observed, it remained at the same position or was even moved to a slightly higher energy: 2,75 keV compared to 2,5 keV. These results combined with the difficulties involved with transferring the graphene lead to the conclusion that graphene is not a viable material to replace TiN as the conductive layer using the described methods. In future research the ALD process to create the alumina layer should be terminated with the TMA step in order to create a better adhesion between the alumina and graphene.

The adhesion of graphene to magnesium oxide membranes proved to be better than to alumina membranes, however the transmission electron yield was much lower than samples with TiN as conductive layer, making graphene again not a viable option to replace TiN. Magnesium oxide can dissolve in water, which made this transfer process not ideal to begin with. Several samples were covered with graphene, but only one attempt was successful. The observed transmission electron yield in this sample was much lower than samples with TiN, 1,3 versus 2,4, and the maximum yield was observed at a higher primary electron energy, 6 keV versus 4,9 keV, instead of the expected lower value. These results might be caused by a thin residual layer of silicondioxide on the membrane. Further research should be done in order to rule this out. For now, the results indicate that graphene is not suitable to replace TiN on magnesium oxide membranes.

The use of ALD to deposit the TiN as conductive layer works well and a 5 nm layer conduct enough electrons to prevent charge up effects in the sample. This means that all layers of the membrane can be deposited in a single session in the ALD, making production easier. In the future more research could be done to the minimize the thickness of this layer, where it still conducts electricity. A thinner TiN layer could give higher transmission yield at a lower primary electron energy.

The transfer-free graphene-alumina method proved to be inconclusive since no working samples were produced. The difficulties that arose due to the copper layer that was involved, proved to be problematic in the production process. The etching of the cavities in the silicon layer was more difficult than was expected beforehand and three out of five wafers were lost during that step. The silicon oxide layer of the single wafer that survived the production process was probably not etched long enough, making it impossible to etch away the copper layer underneath and releasing the membranes. Had this oxide etching been done long enough, some working samples probably would have been created. For future research I would advise to use a thicker silicon oxide layer and etch out the cavities before the copper was deposited, so that the regularly checked and maintained chemical baths could be used. This should result in a much more predictable result than was observed in this research.

Literature

Berman, D., Erdemir, A., & Sumant, A. V. (2014). Graphene: a new emerging lubricant. *Materials Today, 17*(1), 31-42.

Castro Neto, A. H., Guinea, F., Peres, N. M. R., Novoselov, K. S., & Geim, A. K. (2009). The electronic properties of graphene. *Reviews of Modern Physics, 81*(1), 109-162.

Chan, H. W., & Graaf, H. v. d. (not published).

Childres, I., Jauregui, L. A., Park, W., & Chen, H. C. a. Y. P. (2013). Raman Spectroscopy of Graphene and Related Materials>.

Ehrenfreund, P., & Foing, B. H. (2010). Fullerenes and Cosmic Carbon. *Science, 329*, 1159-1160.

Fuchs, J.-N., & Goerbig, M. O. Introduction to the physical properties of graphene.

Lengauer, W., Binder, S., Aigner, K., Ettmayer, P., Guillou, A., Debuigne, J., & Groboth, G. (1995). Solid state properties of group IVb carbonitrides. *Journal of Alloys and Compounds*, 137-147.

Novoselov, K. S., Geim, A. K., Morozov, S. V., Jiang, D., Zhang, Y., Dubonos, S. V., . . . Firsov, A. A. (2004). Electric Field Effect in Atomically Thin Carbon Films. *Science, 306*, 666-669.

Park, D.-W., Mikael, S., Chang, T.-H., Gong, S., & Ma, Z. (2015). Bottom-gate coplanar graphene transistors with enhanced graphene adhesion on atomic layer deposition Al2O3. *Applied Physics Letters, 106*(10), 102106.

Park, Y. H., Kim, M. H., Kim, S. B., Jung, H. J., Chae, K., Ahn, Y. H., . . . Lee, S. W. (2016). Enhanced Nucleation of High-k Dielectrics on Graphene by Atomic Layer Deposition. *Chemistry of Materials, 28*(20), 7268-7275.

Steinsland, E., Finstad, T., & Hanneborg, A. (2000). Etch rates of (100),(111) and (110) single-crystal silicon in TMAH measured in situ by laser reflectance interferometry. *Sensors and Actuators A: Physical, 86*(1-2), 73-80.

Vervuurt, R. H., Karasulu, B., Verheijen, M. A., Kessels, W. E., & Bol, A. A. (2017). Uniform Atomic Layer Deposition of Al2O3 on Graphene by Reversible Hydrogen Plasma Functionalization. *Chemistry of Materials, 29*(5), 2090-2100.\

Wang, L., Travis, J. J., Cavanagh, A. S., Liu, X., Koenig, S. P., Huang, P. Y., Bunch, J. S. (2012). Ultrathin oxide films by atomic layer deposition on graphene. *Nano Letters, 12*(7), 3706-3710.

Wikipedia. (2019). Photomultiplier Tube. Retrieved from https://en.wikipedia.org/wiki/Photomultiplier_tube

Zhang, H., Lee, G., Gong, C., Colombo, L., & Cho, K. (2014). Grain Boundary Effect on Electrical Transport Properties of Graphene. *The Journal of Physical Chemistry C, 118*(5), 2338-2343.

Zheng, L., Cheng, X., Cao, D., Wang, G., Wang, Z., Xu, D., . . . Shen, D. (2014). Improvement of Al2O3 films on graphene grown by atomic layer deposition with pre-H2O treatment. *ACS Appl Mater Interfaces, 6*(10), 7014-7019.

Appendix A – Procedure for Graphene Transfer

This appendix gives an overview of the steps taken to transfer graphene from a wafer to a sample as discussed in chapter 2.

1) PMMA is dissolved in chlorobenzene with a concentration of 46 mg/mL
2) PMMA is spincoated on the wafer at a speed of 1500 rpm for 60 seconds (acceleration of 1000 rpm/s). The resulting PMMA is approximately 2 μm.
3) The wafer is soft baked at 150^{o}C for 60 seconds on a hotplate.
4) The wafer is cut into samples of 1 to 2 cm squared. The bigger the samples are, the longer the Cu etching will take.
5) The sample is put into a 15% $FeCl_3$ solution in H_2O in order to etch the Cu from under the graphene. After the Cu is etched away, the Si/SiO_2 drops, while the PMMA/graphene floats on the surface. (This step can take up to one day depending on the size of the sample).
6) Now the PMMA/graphene is gently scooped out of the $FeCl_3$ solution by a spoon and put in water to dilute the remaining $FeCl_3$. This step can be repeated to dilute the etching solution and clean the sample even further. (A pipet is used to put some drops on the top of the PMMA/Graphene to rinse the surface).
7) 1% HCl is used to remove any metallic particles (PMMA/graphene is scooped out of water into this solution).
8) PMMA/graphene is again scoped out of HCl solution into demineralized water and rinsed.
9) The target sample is held under the surface of the water and is pulled up almost vertically next to the PMMA/graphene, which sticks to the surface. (The graphene should catch on an edge of the target substrate).
10) The sample with PMMA/graphene attached is placed vertical to dry for 20-30 minutes (the water is also pulled from the interface by gravity).
11) The sample is baked on a hotplate first at 60 ^{o}C to prevent steam pressure breaking the membrane. After 5-10 minutes the temperature is raised to 120 ^{o}C in order to dry the sample completely for 5 minutes and facilitate adhesion.
12) The sample is held in acetone at 45 ^{o}C for 10 minutes to dissolve the PMMA.
13) The sample is dried in air to remove the acetone.

Appendix B – SEM Measurements

This appendix provides measurement data belonging to figures 19 and 28 and in chapters 2 and 3. Also some background on the data collection is given as well as the uncertainties of the measurements and calculations.

The measurements were performed in a SEM using a special setup involving a Faraday cup and three Keithley 2450 sourcemeters. These were set up to measure the currents going in and out of the sample. The set up consists of a sample holder, a retarding grid (to apply a bias to differentiate between forward scattered electrons and transmission electrons) and a collector (Faraday cup, see figure 37). Each of these three elements was connected to a Keithley sourcemeter to measure the currents to or from the element, I_{Sample}, I_{Grid} and $I_{Collector}$, respectively. Before each measurement, the electron beam was send through a hole in the sample holder and the measured total current corresponds with the beam current, I_{Beam}. The samples were tested for different electron beam energies ranging from 0,30 keV to 10 keV. Between these measurements the background signal was measured, eliminating any offsets in the set up or the sourcemeters.

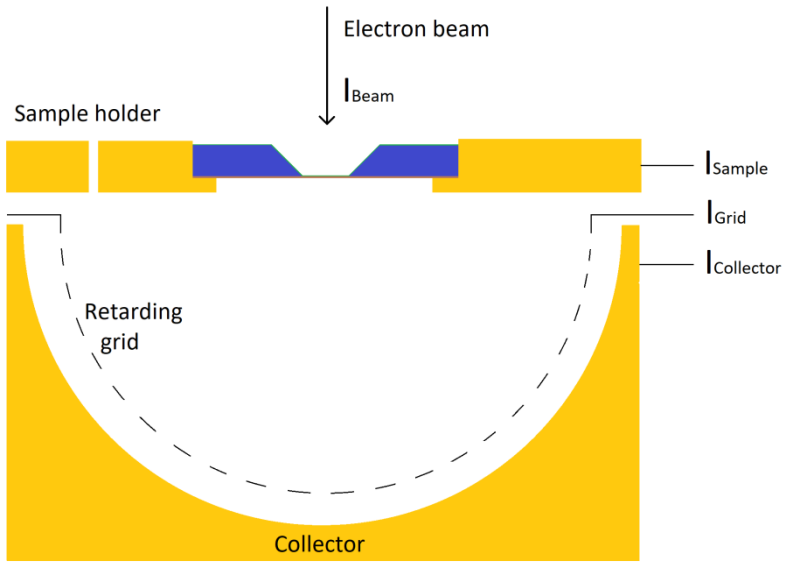

Figure 37. The set up used in these measurements. The sample holder, retarding grid and collector are all connected to a Keithley and the currents through them are measured.

The total current entering the sample is the sum of I_{Beam} and I_{Sample}. After equilibrium is reached, the total current leaving the sample is equal to the current entering the sample. When this is divided by the current of the beam you get the total secondary emission coefficient $\gamma(E)$.

$$\gamma(E) = \frac{I_{Beam} + I_{Sample}}{I_{Beam}} = REY(E) + TEY(E)$$

Here $REY(E)$ is the total reflection electron yield and $TEY(E)$ the total transmission electron yield. The $TEY(E)$ is measured directly by adding the grid current to the collector current and dividing them by the beam current. The $REY(E)$ can be found by calculating the difference between $\gamma(E)$ and $TEY(E)$.

$$TEY(E) = \frac{I_{Grid} + I_{Collector}}{I_{Beam}}$$

$$REY(E) = \frac{I_{Beam} + I_{Sample} - I_{Grid} - I_{Collector}}{I_{Beam}}$$

All of the different currents are measured 20 times per second over a period of 20 seconds. The average current over this period is calculated along with the corresponding standard deviation, making a single measurement point for a specific primary electron energy. Using the calculations described above, combined with uncertainty analysis, the refelection and transmission electron yields are calculated. The results are found in the table below.

Table 1. Measured and processed data belonging to figure 19.

Sputtered TiN (5nm) on 25 nm alumina					Graphene on 25 nm alumina				
E [eV]	*REY*	σ_{REY}	*TEY*	σ_{TEY}	*E [eV]*	*REY*	σ_{REY}	*TEY*	σ_{TEY}
350	1,80	0,1	0,03	2	350	2,21	0,13	0,01	7
550	1,60	0,09	0,02	2	550	1,96	0,13	0,01	4
750	1,42	0,06	0,03	0,8	750	1,71	0,12	0,02	2
950	1,27	0,04	0,13	0,2	950	1,50	0,10	0,12	0,3
1150	1,15	0,05	0,41	0,07	1150	1,32	0,11	0,35	0,11
1350	1,04	0,04	0,79	0,03	1350	1,18	0,11	0,62	0,07
1550	0,96	0,04	1,13	0,02	1550	1,06	0,11	0,86	0,05
1750	0,88	0,04	1,38	0,015	1750	0,96	0,09	1,03	0,03
1950	0,81	0,05	1,55	0,014	1950	0,87	0,09	1,14	0,02
2150	0,74	0,04	1,64	0,01	2150	0,78	0,08	1,21	0,017
2350	0,67	0,04	1,68	0,008	2350	0,71	0,06	1,23	0,012
2550	0,62	0,03	1,69	0,006	2550	0,64	0,06	1,25	0,011
2750	0,56	0,03	1,68	0,006	2750	0,58	0,05	1,26	0,009
2950	0,51	0,03	1,66	0,005	2950	0,53	0,05	1,26	0,007
3150	0,47	0,03	1,63	0,004	3150	0,49	0,04	1,25	0,006
3350	0,43	0,02	1,60	0,004	3350	0,44	0,04	1,25	0,005
3550	0,40	0,02	1,57	0,003	3550	0,41	0,04	1,24	0,005
3750	0,37	0,02	1,54	0,003	3750	0,38	0,04	1,24	0,005
3950	0,35	0,02	1,51	0,003	3950	0,36	0,04	1,23	0,004
4150	0,33	0,02	1,48	0,002	4150	0,34	0,03	1,22	0,004
4450	0,30	0,018	1,44	0,002	4450	0,31	0,03	1,22	0,003
4950	0,27	0,017	1,38	0,0019	4950	0,28	0,03	1,21	0,003
5950	0,22	0,016	1,31	0,0015	5950	0,23	0,03	1,18	0,002
6950	0,18	0,015	1,26	0,0013	6950	0,19	0,02	1,16	0,0015
7950	0,16	0,012	1,22	0,001	7950	0,17	0,02	1,15	0,0012
8950	0,14	0,012	1,19	0,0008	8950	0,15	0,02	1,14	0,0011
9950	0,13	0,012	1,16	0,0008	9950	0,14	0,02	1,12	0,0011

Table 2. Measurement data belonging to figure 27.

Sputtered TiN (5 nm) on 25 nm MgO				
E [eV]	*REY*	σ_{REY}	*TEY*	σ_{TEY}
350	1,05	0,09	0,01	9
550	0,92	0,07	0,01	3
750	0,81	0,04	0,002	5
950	0,68	0,6	0,005	2
1150	0,64	0,03	0,004	1,8
1350	0,58	0,03	0,006	1,1
1550	0,54	0,03	0,006	1,1
1750	0,50	0,02	0,008	0,7
1950	0,47	0,02	0,02	0,3
2150	0,44	0,02	0,06	0,08
2250	0,43	0,02	0,10	0,05
2350	0,42	0,03	0,15	0,03
2450	0,41	0,03	0,23	0,03
2550	0,40	0,04	0,32	0,02
2650	0,39	0,04	0,43	0,02
2750	0,38	0,05	0,56	0,018
2850	0,37	0,06	0,70	0,016
2950	0,37	0,06	0,85	0,014
3050	0,36	0,06	1,00	0,012
3150	0,35	0,06	1,15	0,01
3250	0,34	0,06	1,28	0,009
3350	0,34	0,06	1,41	0,007
3450	0,33	0,06	1,53	0,007
3550	0,33	0,06	1,64	0,006
3650	0,32	0,05	1,74	0,005
3750	0,32	0,05	1,83	0,005
3850	0,31	0,05	1,91	0,004
3950	0,31	0,04	1,97	0,004
4050	0,30	0,04	2,02	0,004
4150	0,29	0,04	2,07	0,003
4350	0,28	0,04	2,12	0,003
4450	0,28	0,04	2,15	0,003
4550	0,27	0,04	2,17	0,003
4750	0,26	0,04	2,19	0,003
4950	0,25	0,04	2,19	0,002
5150	0,24	0,04	2,19	0,002
5350	0,23	0,04	2,17	0,002
5550	0,21	0,04	2,15	0,002
5750	0,20	0,04	2,13	0,002
5950	0,19	0,04	2,10	0,0018
6150	0,18	0,03	2,06	0,0016
6950	0,15	0,03	1,92	0,0013
7950	0,12	0,03	1,75	0,0012
8950	0,10	0,03	1,58	0,001
9950	0,09	0,03	1,39	0,0011

Graphene on 25 nm MgO				
E [eV]	*REY*	σ_{REY}	*TEY*	σ_{TEY}
400	2,23	0,03	0,02	0,9
800	1,78	0,013	0,01	0,4
1200	1,39	0,009	0,01	0,3
1600	1,15	0,009	0,01	0,2
2000	1,00	0,008	0,01	0,2
2400	0,89	0,006	0,01	0,1
2800	0,81	0,006	0,05	0,02
3200	0,73	0,007	0,17	0,01
3600	0,66	0,009	0,373	0,007
4000	0,61	0,012	0,581	0,006
4400	0,57	0,014	0,765	0,005
4800	0,52	0,012	0,921	0,003
5200	0,51	0,008	0,967	0,002
5600	0,44	0,009	1,097	0,0017
6000	0,41	0,01	1,142	0,002
7000	0,39	0,015	1,069	0,004
8000	0,27	0,006	1,146	0,0008
9000	0,21	0,016	1,153	0,002
10000	0,18	0,013	1,123	0,0017